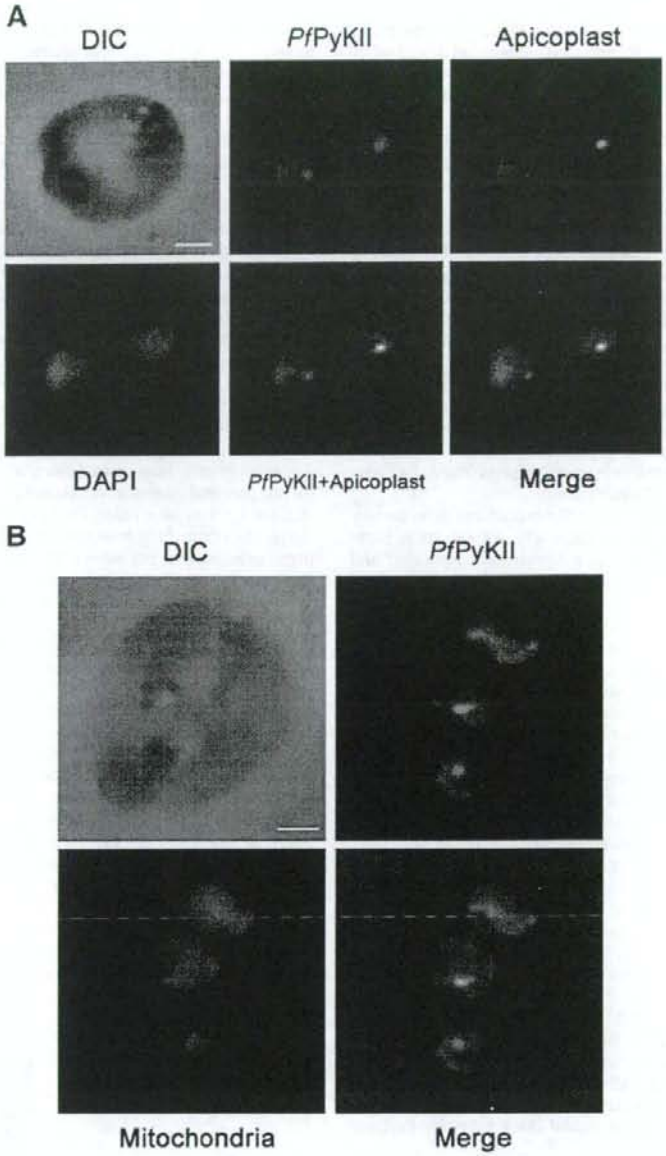

Fig. 3. Immunofluorescent microscopic analysis of co-localization of *Pf*PyKII with the apicoplast, but not with the mitochondrion in red blood cells infected with *P. falciparum*. A: Anti-*Pf*PyKII and anti-*P. falciparum* ACP antibodies detected by AlexaFlour goat anti-mouse 594 (red) and goat anti-rabbit 488 (green) secondary antibodies, respectively. Immunofluoresecnce of *P. falciparum* ACP antibody shows the apicoplast. Merged images indicate co-localization of *Pf*PyKII and *P. falciparum* ACP. Nucleus stained by DAPI (blue). B: Red blood cells infected with parasites expressing citrate synthase fused to GFP targeting the mitochondrion (Tonkin et al. 2004). GFP detected by Cy5-conjugated goat anti-GFP (red). Anti-*Pf*PyKII antibody detected by AlexaFluor goat anti-mouse 488 (green) IgG. Merged image shows that *Pf*PyKII does not co-locate with the mitochondrion. White scale bars are 2 μm.

and *P. falciparum* have comparable organelle components, and were thought to have similar enzyme components in both the apicoplast and the mitochondrion. The pathway differences might reflect differences in intracellular environments or different abilities to import metabolites into those organelles. We expected that the difference in enzymatic properties between *Tg*PyKII and *Pf*PyKII would help in understanding their roles in the two parasites, but several attempts to express the active recombinant enzyme have failed. As pyruvate kinase has been thought to play a role only in glycolysis in the cytosol, pyruvate kinases localized with cell organelles are unique. Non-glycolytic pyruvate kinases have been found only in the apicomplexan parasites, such as *Plasmodium* sp,

Theileria sp. and *T. gondii*. Characterization of non-glycolytic pyruvate kinases would increase the understanding of the unique metabolic pathways in protozoan parasites.

In addition to uncertainty about metabolic pathways, we are also uncertain about the origin of *Pf*PyKII. Although *Pf*PyKII exhibits a typical bipartite signal in the N-terminus, *Pf*PyKII has a proteobacterial origin, which is indicative of the apicoplast protein, and not a cyanobacterial or plastidic origin [2]. We suggest that *Pf*PyKII might have been obtained from endosymbiotic bacteria. Originally *Pf*PyKII may have localized in both the mitochondrion and the apicoplast, as in *T. gondii*; subsequently *P. falciparum* may have lost the mitochondrial location during evolutionary development.

Acknowledgements

We thank Dr. Shinichiro Kawazu (Obihiro University of Agriculture and Veterinary Medical) for providing genomic DNA of *P. falciparum*, and Dr. Geoffrey I. McFadde (University of Melbourne) for providing both anti-acyl carrier protein rabbit antibody and *P. falciparum* expressing citrate synthase fused to GFP. This work was supported in part by Keio Gijuku Academic Development Funds, Japan.

References

[1] Maeda T, Saito T, Oguchi Y, Nakazawa M, Takeuchi T, Asai T. Expression and characterization of recombinant pyruvate kinase from *Toxoplasma gondii* tachyzoites. Parasitol Res 2003;89:259–65.

[2] Saito T, Nishi M, Lim MI, Wu B, Maeda T, Hashimoto H, Takeuchi T, Roos DS, Asai T. A novel GDP-dependent pyruvate kinase isozyme from *Toxoplasma gondii* localizes to both the apicoplast and the mitochondrion. J Biol Chem 2008;283:14041–52.

[3] Chan M, Sim TS. Functional analysis, overexpression, and kinetic characterization of pyruvate kinase from *Plasmodium falciparum*. Biochem Biophys Res Commun 2004;326:188–96.

[4] Sawasaki T, Gouda MD, Kawasaki T, Tsuboi T, Tozawa Y, Takai K, Endo Y. The wheat germ cell-free expression system: methods for high-throughput materialization of genetic information. Methods Mol Biol 2005;310:131–44.

[5] Laemmli UK. Cleavage of structural proteins during the assembly of the head of bacteriophage T4. Nature 1970;227:680–5.

[6] Bradford MM. A rapid and sensitive method for the quantitation of microgram quantities of protein utilizing the principle of protein-dye binding. Anal Biochem 1979;72:248–54.

[7] Tonkin CJ, van Dooren GG, Spurck TP, Struck NS, Good RT, Handman E, Cowman AF, McFadden GI. Localization of organellar proteins in *Plasmodium falciparum* using a novel set of transfection vectors and a new immunofluorescence fixation method. Mol Biochem Parasitol 2004;137:13–21.

[8] Ralph SA, van Dooren GG, Waller RF, Crawford MJ, Fraunholz MJ, Foth BJ, Tonkin CJ, Roos DS, McFadden GI. Tropical infectious diseases: metabolic maps and functions of the *Plasmodium falciparum* apicoplast. Nat Rev Microbiol 2004;2:203–16.

[9] Fleige T, Fischer K, Ferguson DJP, Gross U, Bohne W. Carbohydrate metabolism in the *Toxoplasma gondii* apicoplast: localization of three glycolytic isoenzymes, the single pyruvate dehydrogenase complex, and a plastid phosphate translocator. Eukaryot Cell 2007;6:984–96.

[10] Rigden DJ, Phillips SE, Michels PA, Fothergill-Gilmore LA. The structure of pyruvate kinase form *Leishmania mexicana* reveals details of the allosteric transition and unusual effector specificity. J Mol Biol 1999;291:615–35.

[11] Bendtsen JD, Nielsen H, von Heijne G, Brunak S. Improved prediction of signal peptides: SignalP 3.0. J Mol Biol 2004;340:783–95.

[12] Foth BJ, Ralph SA, Tonkin CJ, Struck NS, Fraunholz M, Roos DS, Cowman AF, McFadden GI. Dissecting apicoplast targeting in the malaria parasite *Plasmodium falciparum*. Science 2003;299(5607):705–8.

Journal of Zoo and Wildlife Medicine 39(3): 370–379, 2008

A SURVEY OF AMOEBIC INFECTIONS AND DIFFERENTIATION OF AN *ENTAMOEBA HISTOLYTICA*–LIKE VARIANT (JSK2004) IN NONHUMAN PRIMATES BY A MULTIPLEX POLYMERASE CHAIN REACTION

Jun Suzuki, Seiki Kobayashi, Ph.D., Rie Murata, Hideo Tajima, D.V.M., Fumitaka Hashizaki, D.V.M., Yoshitoki Yanagawa, D.V.M., Ph.D., and Tsutomu Takeuchi, M.D., Ph.D.

Abstract: A pathogenic *Entamoeba histolytica*–like variant (JSK2004 strain) with genetic variations and a novel isoenzyme pattern isolated from a De Brazza's guenon in a Tokyo zoo in Japan has previously been documented. In this study, a multiplex polymerase chain reaction (PCR) assay that could distinguish the JSK2004-type *E. histolytica*–like variant (JSK04-Eh-V) from *E. histolytica* and *Entamoeba dispar* using three newly designed primer sets for amplifying each specific DNA fragment from their small-subunit ribosomal RNA genes was developed and established. Forty-seven primates (11 species) from the zoo were surveyed by multiplex PCR to assess the prevalence of JSK04-Eh-V infection, which was recognized in six individuals of four species, including an Abyssinian colobus monkey, a De Brazza's guenon (including the individual from whom JSK2004 was isolated), a white-faced saki, and a Geoffroy's spider monkey. In addition, the autopsied individuals of an Abyssinian colobus and Geoffroy's spider monkey that died of amoebic liver abscess were also evaluated. DNA samples were also analyzed for specific genotypes based on the nucleotide sequencing of two protein-coding (chitinase and serine-rich *E. histolytica* protein) genes and the protein-noncoding locus 1-2 that was used for fingerprinting of the *E. histolytica* strain. These studies indicated that the *E. histolytica*–like variant infection in this zoo was caused by the same type (i.e., JSK04-Eh-V). An axenic culture medium (yeast extract–iron–maltose–dihydroxyacetone–serum) was developed based on the yeast extract–iron–gluconic acid–dihydroxyacetone–serum medium, which is designed for axenic culture of *E. dispar*. This new medium could be used for axenically culturing *E. histolytica*, JSK04-Eh-V, and *E. dispar* in a single medium.

Key words: *Entamoeba histolytica*–like variant, multiplex PCR, nonhuman primates, zoo.

INTRODUCTION

Amoebiasis is a zoonotic protozoal infectious disease caused by *Entamoeba histolytica*. The estimated incidence of amoebiasis in humans is approximately 50 million per year, and it has caused nearly 70,000 human deaths.[18] In 1997, *E. histolytica* was reclassified into two species: *E. histolytica* and *Entamoeba dispar* (nonpathogenic); earlier, this differentiation had been difficult to establish because of morphogenetic and phylogenetic similarities.[1,19] This classification is based on the differences in the isoenzyme patterns (zymodemes), the detection of the *E. histolytica*–specific antigen, and *E. histolytica*– and *E. dispar*–specific DNA fragment amplification by polymerase chain reaction (PCR).[3,5]

In Japan, particularly during the last decade, *E. histolytica* infections have not been detected in nonhuman primates by PCR.[12,14] However, three recent articles reported three different pathogenic *E. histolytica*–like variants showing subtle variations in the small-subunit ribosomal RNA (SSU rRNA) gene sequences isolated from cynomolgus monkey (*Macaca fascicularis*),[15] rhesus monkey (*Macaca mulatta*),[13] and De Brazza's guenon (*Cercopithecus neglectus*).[12] The JSK2004-type *E. histolytica* variant (JSK04-Eh-V)[11] has an SSU rRNA gene homology of 99.10% with *E. histolytica* and of 98.47% with *E. dispar*. Previously it was reported that the existing multiplex PCR[2] technique that targeted the specific region of the SSU rRNA gene sequence of *E. histolytica* did not yield the genomic DNA products of an axenic strain (JSK2004) of the *E. histolytica*–like variant from a De Brazza's guenon because of the variation in the nucleotide sequence of the gene.[11]

In the present study, a new multiplex PCR assay that is capable of distinguishing the JSK04-Eh-V

From the Division of Clinical Microbiology, Department of Microbiology, Tokyo Metropolitan Institute of Public Health, 3-24-1, Hyakunin-cho, Shinjuku-ku, Tokyo 169-0073, Japan (Suzuki, Murata, Yanagawa); the Department of Tropical Medicine and Parasitology, School of Medicine, Keio University, 35 Shinanomachi, Shinjuku-ku, Tokyo 160-8582, Japan (Kobayashi, Takeuchi); and the Ueno Zoological Gardens, Ueno-park 9-83, Taito-ku, Tokyo 110-8711, Japan (Tajima, Hashizaki). Correspondence should be directed to Jun Suzuki (Jun_Suzuki@member.metro.tokyo.jp).

Table 1. Oligonucleotide primers used for polymerase chain reaction (PCR) assays in present study.

Primer name		Primer sequence (5' to 3')	Nucleotide position	Accession no.
EnthF	(forward)	ATG GCC AAT TCA TTC AAT GA	198–217	X65163
EnthR	(reverse)	TAC TTA CAT AAA GTC TTC AAA ATG T	648–672	X65163
EhvF	(forward)	ATT TTA TAC ATT TTG AAG ACT TTG CA	642–667	AB426549
EhvR	(reverse)	CTC TAA CCG AAA TTA GAT AAC TAC	1466–1489	AB426549
EhvR2	(reverse)	CAG ATT AAG AAA CAA TGC TTC TTC	1052–1075	AB426549
EntdF	(forward)	GTT AGT TAT CTA ATT TCG ATT AGA AC	1467–1492	AB282661
EntdR	(reverse)	ACA CCA CTT ACT ATC CCT ACC TA	1639–1661	AB282661
EchatF	(forward)	AGG ATT TGT TTT ATA ACA AGT TC	471–493	AF149912
EchatR	(reverse)	AAT AAC CTT TCT CCT TTT TCT ATC	660–685	AF149912
EhartF	(forward)	GTG AAG AGA AAG GAT ATC CAA AGT	221–244	AF149907
EhartR	(reverse)	ATA TCA TTT TCA ACT ACG AGC	623–643	AF149907
Chitinase	(forward)	GGA ACA CCA GGT AAA TGT ATA	466–487	U78319
Chitinase	(reverse)	TCT GTA TTG TGC CCA ATT	799–817	U78319
SREHP	(forward)	GCT AGT CCT GAA AAG CTT GAA GAA GCT G	258–286	M80910
SREHP	(reverse)	GGA CTT GAT GCA GCA TCA AGG T	784–806	M80910
R1 (locus1–2)	(forward)	CTG GTT AGT ATC TTC GCC TGT	1–21	AF276055
R2 (locus1–2)	(reverse)	CTT ACA CCC CCA TTA ACA AT	383–401	AF276055

from *E. histolytica* and *E. dispar* was designed, and the prevalence of JSK04-Eh-V infection in the primates of a zoo in Japan was surveyed using this assay. In addition, the identity of the JSK04-Eh-V strains in the zoo, determined by analyzing their polymorphic genotypes as a fingerprint for identifying the strain of *E. histolytica*, was investigated.

Moreover, the incidence of other amoebic infections in primates was investigated, and the first axenic culture medium that would support the growth of *E. histolytica*, JSK04-Eh-V, and *E. dispar* in a single medium was designed.

MATERIALS AND METHODS

Primates

In order to assess the prevalence of infection with JSK04-Eh-V, 47 captive individuals of 11 primate species from the Tokyo Zoo in Japan, where JSK2004 (JSK04-Eh-V) had been isolated from a De Brazza's guenon, were surveyed.[11] The primates, comprising 11 species, included three De Brazza's guenons (*Cercopithecus neglectus*), 11 Abyssinian colobus monkeys (*Colobus guereza*), two ring-tailed lemurs (*Lemur catta*), two mandrills (*Mandrillus sphinx*), one lesser slow loris (*Nycticebus pygmaeus*), two ruffed lemurs (*Varecia variegata*), one northern night monkey (*Aotus trivirgatus*), seven Geoffroy's spider monkeys (*Ateles geoffroyi*), 12 Japanese macaques (*Macaca fuscata*), five white-faced sakis (*Pithecia pithecia*), and one cotton-top tamarin (*Saguinus oedipus*). Each primate species was housed independently.

Microscopic examination and detection of the *E. histolytica*–specific antigen

Stool samples from each living individual were collected once daily for 3 days from 45 primates to obtain three samples per individual. Prior to performing the multiplex PCR, all stool specimens were examined microscopically after concentrating the *Entamoeba* cysts by the formalin–ether sedimentation technique.[10] The specimens were also examined using an *E. histolytica*–specific antigen detection kit (*E. histolytica II* kit; TechLab, Blacksburg, Virginia 24060, USA). Tissue samples obtained from the primates that had liver abscesses were embedded in paraffin, stained with periodic acid–Schiff, and were examined for amoebae.

DNA preparation

Of the three stool specimens collected from each individual, the specimen that had the largest number of amoebic cysts was utilized for DNA preparation. The cysts were concentrated and partially purified using the modified formalin–ether sedimentation method, in which formalin was replaced with a phosphate-buffered solution (pH 7.4). Subsequently, the QIAamp® DNA stool mini-kit (Qiagen GmbH, Hilden 40724, Germany; catalog no. 51504) was used to isolate the genomic DNAs of amoebae. The genomic DNAs of the amoebae found in the two samples of abscesses obtained from the liver abscess of both the autopsied Abyssinian colobus monkey and Geoffroy's spider monkey that died of amoebic liver abscess; the two ref-

Figure 1. Polymerase chain reaction (PCR) products of the DNA samples from *Entamoeba histolytica*, JSK2004-type *E. histolytica*–like variant (JSK04-Eh-V), and *Entamoeba dispar* differentiated by multiplex PCR. Lane 1: mixture of the DNA templates of lanes 2, 3, and 4; Lane 2: DNA of HM-1:IMSScl6 (*E. histolytica*; length, 475 base pairs [bp]); Lane 3: DNA of JSK2004 clone 2 (JSK2004cl2; JSK04-Eh-V; length, 848 bp); Lane 4: DNA of SAW1734RclAR (*E. dispar*; length, 195 bp); Lane 5: Human *E. histolytica* DNA sample (pus from liver abscess); Lane 6: Human *E. histolytica* DNA sample (stool); Lane 7: JSK04-Eh-V DNA sample (pus from liver abscess) from a Geoffroy's spider monkey; Lane 8: JSK04-Eh-V DNA sample (stool) from a De Brazza's guenon; Lane 9: Human *E. dispar* DNA sample (stool); and Lane 10: *E. dispar* DNA sample (stool) from a De Brazza's guenon.

erence amoebic strains, HM-1:IMSS clone 6 (HM-1:IMSScl6 strain; *E. histolytica*) and SAW1734R clone AR (SAW1734RclAR strain; *E. dispar*), that were kindly supplied by Dr. Lois S. Diamond (National Institutes of Health); and the JSK2004 clone 2 (JSK2004cl2; JSK04-Eh-V) were isolated using the QIAamp DNA mini-kit (Qiagen GmbH; catalog no. 51304).

Primers for multiplex PCR

The primers for multiplex PCR were designed based on the two SSU rRNA gene sequences of HM-1:IMSScl6 (*E. histolytica*; GenBank accession no. X65163) and SAW1734RclAR (*E. dispar*; GenBank accession no. AB282661) and the previously reported sequence of JSK2004cl2 (JSK04-Eh-V; GenBank accession no. AB426549). The three primer sets that were designed—EnthF/EnthR for *E. histolytica*, EntdF/EntdR for *E. dispar*, and EhvF/EhvR for JSK04-Eh-V—are listed in Table 1.

Primer specificity was tested by conducting multiplex PCR on seven other intestinal parasitic protozoan and one nonprotozoan species: axenic trophozoites of *Entamoeba moshkovskii* (Laredo strain), *Entamoeba invadens* (IP-1 strain; ATCC no. 30994), and *Giardia intestinalis* (Portland-1 strain; ATCC no. 30888); cyst forms of *Escherichia coli* and *Cryptosporidium hominis*; culture form of *Blastocystis hominis* (nonprotozoan species) from human stool samples; and *E. coli*, *Entamoeba chattoni*, and *Entamoeba hartmanni* obtained from the stool samples of nonhuman primates.

Multiplex PCR

Amplification was performed in a reaction mixture (50 μl) containing 100 ng of the DNA samples, 25 μl of 2× Multiplex PCR Master Mix (Qiagen GmbH; catalog no. 206143), and 2 μl of each primer at 10 mM. The touchdown method was used for thermal cycling. The cycling conditions were as follows: 15 min at 95°C followed by 40 cycles of denaturation at 94°C for 30 sec, annealing for 40 sec beginning at 61°C and ending at 56°C, and extension at 72°C for 1 min. The annealing temperature was lowered by 1°C after every four cycles until it reached 56°C, after which the same temperature was maintained until the end of the cycling process.

Semi-nested PCR for SSU rRNA

In cases in which a minimal PCR product from the DNA of JSK04-Eh-V was obtained, a semi-nested PCR using the primer set EhvF/EhvR2 was performed (Table 1). For this second PCR (semi-nested PCR), amplification was performed in a reaction mixture (50 μl) containing 1 μl of the first PCR product, 1.0 U of ex*Taq*DNA polymerase (Takara Bio, Inc., Seta, Shiga 520-2134, Japan; catalog no. RR001A), 0.4 μM of each primer, and 0.25 mM of deoxynucleoside triphosphate. The follow-

Table 2. The results of the surveillance for the prevalence of the JSK2004 type *Entamoeba histolytica*-like variant (JSK04-Eh-V) by a newly designed multiplex polymerase chain reaction (PCR) and microscopic examination in a zoo of Tokyo, Japan.

Primate species	Common name	No. of samples	Positive number by multiplex PCR (symptoms)			Antigen detection[a]	Microscopic examination[b]
			Entamoeba histolytica	JSK04-Eh-V	*Entamoeba dispar*		
Old World monkeys							
Cercopithecus neglectus	De Brazza's guenon	3	0	1 (Asymptomatic)	2	1	*E. coli* (3), *E. nana* (2)
Colobus guereza	Abyssinian colobus	11	0	2 (ALA,[c] asymptomatic)	2	1	*E. coli* (8), *E. nana* (3), *G. intestinalis* (4)
Macaca fuscata	Japanese macaque	12	0	0	2	0	*E. chattoni* (7), *E. coli* (2), *E. hartmanni* (5)
Mandrillus sphinx	Mandrill	2	0	0	0	0	*E. chattoni* (1), *E. nana* (1)
Lemur catta	Ring-tailed lemur	2	0	0	0	0	*G. intestinalis* (2)
Varecia variegata	Ruffed lemur	2	0	0	0	0	—
Nycticebus pygmaeus	Lesser slow loris	1	0	0	0	0	—
New World monkeys							
Aotus trivirgatus	Northan night monkey	1	0	0	0	0	*C. mesnili* (1)
Ateles geoffroyi	Geoffroy's spider monkey	7	0	1 (Colitis)	1	0	—
Pithecia pithecia	White-faced saki	5	0	2 (ALA,[c] asymptomatic)	1	2	*G. intestinalis* (1), *E. coli* (1), *E. nana* (1)
Saguinus oedipus	Cotton-top tamarin	1	0	0	0	0	—
Total		47	0	6	8	4	

[a] *E. histolytica*-specific antigen detection kit [*E. histolytica II* kit (TechLab)] was used for examination of stool samples.

[b] *E. coli*: *Entamoeba coli*; *E. nana*: *Endolimax nana*; *G. intestinalis*: *Giardia intestinalis*; *E. chattoni*: *Entamoeba chattoni*; *C. mesnili*: *Chilomastix mesnili*. *E. chattoni* and *E. hartmanni* were identified by PCR. The numbers within the parentheses represent the number of positive cases..

[c] ALA, amebic liver abscess (death).

Figure 2. Differentiated polymerase chain reaction (PCR) products of the DNA samples of *Entamoeba chattoni* and *Entamoeba hartmanni* using PCRs. Lane 1: The product (length, 215 base pairs [bp]) from an *E. chattoni* DNA sample (stool) from a mandrill; Lane 2: The product (length, 215 bp) from an *E. chattoni* DNA sample (stool) from a Japanese macaque; Lane 3: The product (length, 423 bp) from an *E. hartmanni* DNA sample (stool) from a Japanese macaque.

ing cycling parameters were utilized: *Taq* activation at 94°C for 3 min; 35 cycles of denaturation at 94°C for 40 sec, annealing at 58°C for 40 sec, and extension at 72°C for 1 min; and extension at 72°C for 5 min.

PCR for *E. chattoni* and *E. hartmanni*

Entamoeba chattoni and *E. hartmanni* were identified by PCR assays using two primer sets (i.e., EchatF/EchatR[16] and EhartF/EhartR, respectively) (Table 1). For *E. hartmanni*, a newly designed primer set based on its SSU rRNA sequence (GenBank accession no. AF149907) was used. These amplifications were performed in a reaction mixture (50 μl) containing 100 ng of the DNA sample, 1.0 U of LA*Taq*DNA polymerase, 0.4 μM of each primer, and 0.25 mM of deoxynucleoside triphosphate. The following cycling parameters were utilized: *Taq* activation at 94°C for 3 min; 35 cycles of denaturation at 94°C for 40 sec, annealing at 55°C for 40 sec, and extension at 72°C for 1 min; and extension at 72°C for 5 min.

Polymorphic gene analysis

The genotyping of JSK04-Eh-V was reexamined to determine whether it would have the same genotype as JSK2004cl2. This was performed based on the nucleotide sequences of two protein-coding (chitinase and SREHP) genes and the protein-noncoding locus 1-2[4,7,20] that was used as a fingerprint for identifying the *E. histolytica* strain. The primers used are shown in Table 1. These amplifications were performed in a reaction mixture (50 μl) containing 100 ng of the DNA sample, 1.0 U of LA*Taq*DNA polymerase (Takara Bio, Inc.; catalog no. RR02AG), 0.4 μM of each primer, and 0.25 mM of deoxynucleoside triphosphate. The following cycling parameters were utilized: *Taq* activation at 94°C for 3 min; 35 cycles of denaturation at 94°C for 40 sec, annealing at 50°C (chitinase, SREHP, and locus 1-2) or 56°C (SSU rRNA) for 40 sec, and extension at 72°C for 1 min; and extension at 72°C for 5 min.

Sequence analysis

Sequence analysis was performed. The multiplex PCR products of SSU rRNA; the PCR products of chitinase, SREHP, and the locus 1-2 genes from the JSK04-Eh-V isolates; and the PCR products of SSU rRNA from *E. chattoni* and *E. hartmanni* were sequenced using the ABI Prism BigDye Terminator v3.1 Cycle Sequencing Ready Reaction Kit (Applied Biosystems, Foster City, California 94404, USA; catalog no. 4337455) and an ABI PRISM 3100 Genetic Analyzer.

Yeast extract–iron–maltose–dihydroxyacetone–serum (YIMDHA-S) medium

An axenic culture medium, namely, YIMDHA-S, based on the yeast extract–iron–gluconic acid–dihydroxyacetone–serum medium (YIGADHA-S)[6] designed for the axenic culture of *E. dispar*, was designed for the isolation and culture of *E. histolytica*, the *E. histolytica*–like variant, and *E. dispar* in a single medium. YIGADHA-S differs from the existing YIMDHA-S medium in that gluconic acid, 0.5% in YIGADHA-S, is replaced with an equal concentration of maltose in YIMDHA-S. Another significant issue related to this culture system is that the growth of amoebae in YIMDHA-S is largely affected by the quality of the yeast extract. Accordingly, the effectiveness of several commercially available yeast extracts purchased from different manufacturers as an ingredient of YIMDHA-S was evaluated. Except for the standard stock obtained from BBL (Becton Dickinson Co., Cockeysville, Maryland 21030, USA; catalog no. 4311929; lot no. 1000I9DHJT), among all the yeast extracts test-

Figure 3. Comparison of the chitinase sequences of the *Entamoeba histolytica*–like variant strain JSK2004cl2 and *E. histolytica*–like variants detected from *Ateles geoffroyi* and *Pithecia pithecia* with the sequences of the reference *E. histolytica*–like variant strain isolated from *Macaca fascicularis*. JSK2004cl2: The sequence of the chitinase gene of DNA from JSK2004cl2 obtained from a De Brazza's guenon (GenBank accession no. AB426705). *Samples: The chitinase gene sequences of DNA samples from a Geoffroy's spider monkey (one pus sample from a liver abscess) and white-faced saki (two stool samples); EHMfas1: the chitinase gene sequences (GenBank accession no. AB282755) of the DNA of an isolate of another type of *E. histolytica*–like variant isolated from a cynomolgus monkey.[15]

ed, only that obtained from Merck (Merck KGaA, Damstadt 64271, Germany; catalog no. 1.03753; lot no.VM510453 539) was effective for constant subculture of the axenic strains of *E. histolytica* (HM-1:IMSScl6), *E. dispar* (AS16 IR isolated from human samples and CYNO 09:TPC isolated from the cynomolgus monkey [*Macaca fascicularis*]),[6] and JSK04-Eh-V (JSK2004) from the De Brazza's guenons that were subjected to a trial of axenic cultivation.

RESULTS

Specificity of multiplex PCR

Each PCR product from the genomic DNA of each of the axenic strains of *E. histolytica* (HM-1: IMSScl6), JSK04-Eh-V (JSK2004cl2), and *E. dispar* (SAW1734clAR) analyzed by multiplex PCR was obtained independently; the lengths of the fragments were 475 base pairs (bp), 848 bp, and 195 bp, respectively (Fig. 1), which was confirmed by individual nucleotide sequencing. The findings of multiplex PCR were reproducible during the practical trials using amoebic DNAs isolated from the stool samples and liver abscesses of humans and nonhuman primates infected with *E. histolytica*, JSK04-Eh-V, and *E. dispar* (Fig. 1). The specificity of multiplex PCR was examined by analyzing the templates of the DNA extracted from seven other intestinal parasitic protozoan and one nonprotozoan species, as previously described. None of the PCR products was observed on multiplex PCR examination of these parasites.

Sensitivity of multiplex PCR and semi-nested PCR

The sensitivity of multiplex PCR was found to be at least 200 cysts/100 mg of the stool sample for JSK04-Eh-V and 100 cysts/100 mg of the stool samples for *E. histolytica* and *E. dispar*. In an attempt to assess the sensitivity of the technique for mixed infections, 400 cysts or trophozoites of JSK04-Eh-V could be detected and differentiated in the presence of 100 cysts/100 mg of the stool samples for *E. histolytica* and *E. dispar*.

Semi-nested PCR using the primer set EhvF/EhvR2 detected 50 cysts/100 mg stool sample for JSK04-Eh-V. In one case of the white-faced saki, in which a minimal PCR product from the DNA of JSK04-Eh-V was obtained, semi-nested PCR yielded the 434-bp–long PCR product.

```
JSK2004cl2 AAG AAA AAG AAA AAA GTA GCT CAG CAA AAC CAG AAT CAA GTT CAA ACA AAG ATA ATG AAG
EHMfas1     ... ... ... ... ... ... ... ... ... ... ... ... ... ... ... ... ... ... ...
P19         ... ... ... ... ... ... ... ... ... ... ... ... ... ... ... ... ... ... ...

JSK2004cl2 ATG AGG AAG ATG AAG ATG AAG ATG ATG AAG AAG ATG AAG ATG AGA ATG AAA AAG CAA GTT
EHMfas1     ... .-- --- -G. ... ... ... ... ... ... ... ... ... ... ... ... ... ... ...
P19         ..A .-- --- -.. ... ..A .T. .A. ... .G. ... ... ... ... ... ... ... ... ...

JSK2004cl2 CAA GTG ATA AAT CAG AAG CAA GTT CAA GTG ATA AAT CAG A--- --- --- --- -AT CAA GCT
EHMfas1     ... ... ... ... ... ... ... ... ... ... ... ... ..C ... .TA ACA AAC CAG A.G ... ...
P19         ... ... ... ... ... ... ... .C. ... ... ... ... ..C ... .-- --- --- --- -.G ... .T.

JSK2004cl2 CAA ATG ATA AAT CAG AAT CAA GCT CAA ATG ATA AAC CAG AAT CAA GCT CAA ATG ATA AAC
EHMfas1     ... G.. ... ..C ... ..G ... ... ... G.. ... ... ... ..G ... .T. ... G.. ... ...
P19         ... G.. ... ..C ... ..G ... .T. ... G.. ... ... ... ..G ... .T. ... G.. ... ...

JSK2004cl2 CAG AAG CAA GTT CAA GTG ATA AAT CAG AAG CAA GTT CAA GTG ATA AAC CAG ATA ACA AAC
EHMfas1     ... .-- --- --- --- -.A .C. ..C ... ... ... ... ... ... ... ... ... ... ...
P19         ... .-- --- --- --- -.A .C. ..C ... ... ... ... ... ... ... ... ... ... ...

JSK2004cl2 CAG AAG CAA GTT CAA GTG ATA AAC CAG ATA ACA AAC CAG AAG CAA GTT CAA GTG ATA AAC
EHMfas1     ... ... ... .C. ... ... ... ... ... ... ... ... ... ... ... ... ... ... ...
P19         ... ... ... ... ... ... ... ... ... ... ... ... ... ... ... .C. ... ... ...

JSK2004cl2 CAG ATA ACA AAC CAG AAG CAA GTT CAA GTG ATA AGC CAG ATA ACA AAC CAG AAG CAA GCT
EHMfas1     ... ... ... ... ... ... ... .C. ... ... ... .A. ... ... ... ... ... ... ...
P19         ... ... ... ... ... ... ... .C. ... ... ... .A. ... ... ... ... ... ... .T.

JSK2004cl2 CAA CTA ATA AAC CAG AAG CAA GTT CAA CTA ATA AAC CAG AAG CAA GTT CAA CTA GTA ATT
EHMfas1     ... ... ... ... ... ... ... ... ... ... ... ... ... ... ... ... ... ... ...
P19         ... ... ... ... ... ... ... ... ... ... ... ... ... ... ... ... ... ... ...

JSK2004cl2 CAA -TG ATA AAT CAG AAA GTA GTT CAG ATA ATG ATA ATA ATA (GenBank.:AB426706)
EHMfas1     ... A.. ... ... ... ... ... ... ... ... ... ... ... ... ... (GenBank.:AB197935)
P19         ... A.. ... ... ... ... ... ... ... ... ... ... ... ... ... (GenBank :AB282662)
```

Figure 4. Comparison of the sequences in the SREHP of the *Entamoeba histolytica*–like variant JSK2004cl2 strain with the reference *E. histolytica*–like variant strains isolated from *Macaca fuscicularis* and *Macaca mulatta*. JSK2004cl2: The sequence of the serine-rich *E. histolytica* protein (SREHP) gene in the DNA of JSK2004cl2 from a De Brazza's guenon (GenBank accession no. AB426706); EHMfas1: the sequences of the SREHP gene (GenBank accession no. AB197935) in the DNA of an isolate of another type of *E. histolytica*–like variant isolated from a cynomolgus monkey;[15] P19: the sequence of the SREHP gene (GenBank accession no. AB282662) in the DNA of another type of *E. histolytica*–like variant (an established strain) isolated from a rhesus monkey.[13]

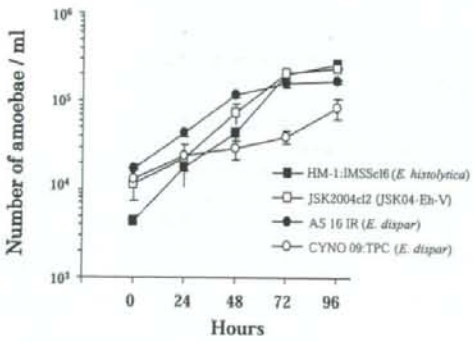

Figure 5. The growth kinetics of the axenically cultured HM-1:IMSScl6, JSK2004cl2, AS 16 IR, and CYNO 09:TPC strains in the yeast extract–iron–maltose–dihydroxyacetone–serum (YIMDHA-S) medium. The mean numbers of amoebae in duplicate cultures have been plotted.

Prevalence of amoebic infections in the zoo

Since a pathogenic JSK04-Eh-V strain was isolated from De Brazza's guenons in the Tokyo zoo, the prevalence of JSK04-Eh-V infection was surveyed using multiplex PCR and was detected in six individuals of four primate species: Abyssinian colobus monkey; De Brazza's guenon, including the individual from which JSK2004 was isolated; white-faced saki; and Geoffroy's spider monkey. In addition, the autopsied samples of the Abyssinian colobus monkey and Geoffroy's spider monkey that died of amoebic liver abscess were positive for JSK04-Eh-V. Among the primates of the zoo, the infection rates with *E. histolytica*, *E. dispar*, and JSK04-Eh-V were 0% (0/47), 17% (8/47), and 13% (6/47), respectively (Table 2). Mixed infection with *E. dispar* and JSK04-Eh-V was not detected by multiplex PCR. The prevalence of the other species of amoebae examined microscopically (i.e., *E. coli* and *Endolimax nana*), were 30% (14/47) and 15%

(7/47), respectively. The prevalence of *E. chattoni* and *E. hartmanni* examined microscopically and by PCR was 17% (8/47) and 11% (5/47), respectively (Table 2); their fragments were confirmed by nucleotide sequencing and corresponded to the sequence dates of *E. hartmanni* (GenBank accession no. AF149907) and *E. chattoni* (GenBank accession no. AF149912). The amplified PCR products are shown in Figure 2.

Polymorphic genes in JSK04-Eh-V isolates

Genotyping based on the nucleotide sequencing of the chitinase, SREHP, and locus 1-2 genes was applied to the genotyping of JSK04-Eh-V. The DNA samples of JSK04-Eh-V from each of the six primates were subjected to PCR to detect the fragments of the chitinase, SREHP, and locus 1-2 genes. The PCR products of the chitinase genes from the DNA samples of two primates and JSK2004cl2 and the PCR products of the locus 1-2 genes from the DNA samples of four primates and JSK2004cl2 were sequenced; however, the PCR products of the SREHP genes were obtained only from the DNA sample of JSK2004cl2. There was perfect homology between the sequences of the PCR products of the chitinase genes obtained from two primates (one Geoffroy's spider monkey and one white-faced saki) and the PCR products of the locus 1-2 genes from four primates (two Abyssinian colobus monkeys, one Geoffroy's spider monkey, and one white-faced saki). Moreover, the sequences of the two genes of JSK2004cl2 (locus 1-2: GenBank accession no. AB426704; chitinase: GenBank accession no. AB426705) also demonstrated perfect homology. However, the sequence data of the chitinase and SREHP genes of the other two types of *E. histolytica*–like variants (GenBank accession nos. AB282755 and AB197935) isolated from the cynomolgus and rhesus monkeys were different compared to the sequence data of the chitinase gene and SREHP gene (GenBank accession no. AB426706) of JSK2004cl2 (Figs. 3, 4).

Growth kinetics of amoebae in YIMDHA-S

The growth kinetics of axenically grown *E. histolytica* (HM-1:IMSScl6), *E. dispar* (AS 16 IR and CYNO 09:TPC), and JSK04-Eh-V (JSK2004) in YIMDHA-S are shown in Figure 5. These established axenic strains adapted to the YIMDHA-S culture conditions within three subcultures; thereafter, they were inoculated into the YIMDHA-S from the classic TYI-S-33[3] (HM-1:IMSScl6) or YIGADHA-S (AS 16 IR and CYNO 09:TPC) media.

DISCUSSION

The multiplex PCR for *E. histolytica*, JSK04-Eh-V, and *E. dispar* permits species identification in a single reaction mixture and is, therefore, more cost effective and useful for prevention of contamination of DNA samples.

Surveillance of the prevalence of JSK04-Eh-V infection among the primates in the zoo was conducted using multiplex PCR for differential diagnosis of *E. histolytica*, JSK04-Eh-V, and *E. dispar*. Multiplex PCR was confirmed as a useful method for the detection and identification of *E. histolytica*, JSK04-Eh-V, and *E. dispar* in nonhuman primates and even in the zookeepers who were in contact with the primates, because the specificity and reproducibility of this technique were adequate for efficient surveillance of JSK04-Eh-V in the present study.

Concerning the microscopic stool examination process in this survey, amoebic cysts or trophozoites were not always detected in every stool sample obtained from individuals infected with JSK04-Eh-V and *E. dispar*. These cysts or trophozoites could be detected only in one third to two thirds of the stool samples, despite the collection of samples from each individual primate once a day for 3 days. The results indicated that performing a stool examination per day (at least three times) on alternate days is necessary.

The JSK04-Eh-V strain of *E. histolytica* was detected by using the *E. histolytica II* kit, an *E. histolytica*–specific antigen (adhesin) detection kit. It is reported that one of the factors determining the pathogenicity of *E. histolytica* is the cytolysis of host cells that begins with the adhesion of the amoebae to the mucosal target cells of the large intestine via galactose/*N*-acetyl D-galactosamine-inhibitable (Gal/GalNAc) lectin.[8,9] The detection of the *E. histolytica*–specific antigen from JSK04-Eh-V by using the *E. histolytica II* kit indicated that the Gal/GalNAc lectin structure in JSK04-Eh-V is identical to that in *E. histolytica*.

Although the nucleotide sequence of the polymorphic SREHP gene from five primates, except for JSK2004cl2, could not be amplified by PCR, the polymorphic chitinase and locus 1-2 gene sequences from three and six primates, respectively, were observed to be identical. The reasons for the inability of PCR to amplify the SREHP gene were thought to be related to the small amount of JSK04-Eh-V DNA in the stool and liver abscess samples, which were insufficient for the PCR, and the presence of a few irrelevant PCR fragments in each case. Therefore, JSK04-Eh-V infections that oc-

curred in the zoo was presumed to have been spread by a single strain, because the infection was limited to primate groups within a particular zone of the zoo at around the same time. The route of transmission of the infection from the isolated group of primates in captivity, including individuals infected with JSK04-Eh-V, to the other groups has not been determined. It is possible that the cysts are the causative agents of JSK04-Eh-V infection, because *E. histolytica* cysts have been reported to be capable of surviving and retaining their infectivity for a month under appropriate wet conditions.[17]

The symptoms of the zoo primates infected with JSK04-Eh-V differed considerably depending on their species; the symptoms in the De Brazza's guenon were relatively mild, while symptoms in the Abyssinian colobus monkey and Geoffroy's spider monkey were severe and fatal. There appear to be species-specific differences among the primates with regard to susceptibility. Although the transmission route was not clear, it is possible that the primates may be carriers and may thus be a source of the parasite. Prior to this study, JSK04-Eh-V infection was thought to have been eradicated, owing to the diligence of the veterinarians and zookeepers working in the zoo, and, fortunately, no zoonotic infection (including amoebiasis) was found among the zookeepers.

YIMDHA-S was designed for the axenic culture of *E. histolytica*, JSK04-Eh-V, and *E. dispar*. This medium is considered to be efficient in comparing biological characteristics of JSK04-Eh-V with *E. histolytica* and *E. dispar*, such as the intensity of in vitro virulence to mammalian tissue culture cell lines,[9] in a single medium under the same culture conditions.

Acknowledgment: A part of this work was supported by a Health Sciences Research Grant-in-Aid for Emerging and Reemerging Infectious Diseases from the Ministry of Health, Labour and Welfare of Japan.

LITERATURE CITED

1. Diamond, L. S., and C. G. Clark. 1993. A redescription of *Entamoeba histolytica* Schaudinn, 1903 (Emended Walker, 1911) separating it from *Entamoeba dispar* Brumpt, 1925. J. Eukaryot. Microbiol. 40(3): 340–344.

2. Diamond, L. S., D. R. Harlow, and C. C. Cunnick. 1978. A new medium for the axenic cultivation of *Entamoeba histolytica* and other *Entamoeba*. Trans. R. Soc. Trop. Med. Hyg. 72(3): 431–432.

3. Evangelopoulos, A., G. Spanakos, E. Patsoula, N. Vakalis, and N. Legakis. 2000. A nested, multiplex, PCR assay for the simultaneous detection and differentiation of *Entamoeba histolytica* and *Entamoeba dispar* in faeces. Ann. Trop. Med. Parasitol. 94: 233–240.

4. Ghosh, S., M. Frisardi, L. Ramirez-Avila, S. Descoteaux, K. Sturm-Ramirez, O. A. Newton-Sanchez, J. I. Santos-Preciado, C. Ganguly, A. Lohia, S. Reed, and J. Samuelson. 2000. Molecular epidemiology of *Entamoeba* spp.: evidence of a bottleneck (demographic sweep) and transcontinental spread of diploid parasites. J. Clin. Microbiol. 38: 3815–3821.

5. Haque, R., I. K. Ali, S. Akther, and W. A. Petri, Jr. 1998. Comparison of PCR, isoenzyme analysis, and antigen detection for diagnosis of *Entamoeba histolytica* infection. J. Clin. Microbiol. 36: 449–452.

6. Kobayashi, S., E. Imai, A. Haghighi, S. A. Khalifa, H. Tachibana, and T. Takeuchi. 2005. Axenic cultivation of *Entamoeba dispar* in newly designed yeast extract-iron-gluconic acid-dihydroxyacetone-serum medium. J. Parasitol. 91: 1–4.

7. Li, E., C. Kunz-Jenkins, and S. L. Stanley, Jr. 1992. Isolation and characterization of genomic clones encoding a serine-rich *Entamoeba histolytica* protein. Mol. Biochem. Parasitol. 50(2): 355–357.

8. Petri, W. A., Jr., R. D. Smith, P. H. Schlesinger, C. F. Murphy, and J. I. Ravdin. 1987. Isolation of the galactose-binding lectin that mediates the in vitro adherence of *Entamoeba histolytica*. J. Clin. Invest. 80: 1238–1244.

9. Ravdin, J. I., and R. L. Guerrant. 1982. Separation of adherence, cytolytic, and phagocytic events in the cytopathogenic mechanisms of *Entamoeba histolytica*. Arch. Invest. Med. 13: 123–128.

10. Ritchie, L. S. 1948. An ether sedimentation technique for routine stool examinations. Bull. U. S. Army Med. Dept. 8: 326.

11. Suzuki, J., S. Kobayashi, R. Murata, Y. Yanagawa, and T. Takeuchi. 2007. Profile of a pathogenic *Entamoeba histolytica*-like variant with variations in the nucleotide sequence of the small subunit ribosomal RNA isolated from a primate (De Brazza's Guenon). J. Zoo Wildl. Med. 38(3): 471–474.

12. Tachibana, H., X. J. Cheng, S. Kobayashi, N. Matsubayashi, S. Gotoh, and K. Matsubayashi. 2001. High prevalence of infection with *Entamoeba dispar*, but not *E. histolytica*, in captive macaques. Parasitol. Res. 87: 114–117.

13. Tachibana, H., T. Yanagi, K. Pandey, X. J. Cheng, S. Kobayashi, J. B. Sherchand, and H. Kanbara. 2007. An *Entamoeba* sp. strain isolated from rhesus monkey is virulent but genetically different from *Entamoeba histolytica*. Mol. Biochem. Parasitol. 153(2): 107–114.

14. Takano, J., T. Narita, H. Tachibana, T. Shimizu, H. Komatsubara, K. Terao, and K. Fujimoto. 2005. *Entamoeba histolytica* and *Entamoeba dispar* infections in cynomolgus monkeys imported into Japan for research. Parasitol. Res. 97: 255–257.

15. Takano, J., T. Narita, H. Tachibana, K. Terao, and K. Fujimoto. 2007. Comparison of *Entamoeba histolytica* DNA isolated from a cynomolgus monkey with human isolates. Parasitol. Res. 101(3): 539–546.

16. Verweij, J. J., A. M. Polderman, and C. G. Clark. 2001. Genetic variation among human isolates of uninu-

cleated cyst-producing *Entamoeba* species. J. Clin. Microbiol. 39(4): 1644–1646.

17. Walsh, J. A. 1988. Transmission of *Entamoeba histolytica* infection. *In:* Amebiasis. Wiley Medical, John Wiley and Sons, Inc., New York, New York. Pp. 106–126.

18. World Health Organization. 1995. The World Health Report 1995: Bridging the Gaps, vol. 16. World Health Organization, Geneva, Switzerland. Pp. 28–29.

19. World Health Organization. 1997. Amoebiasis. W. H. O. Wkly. Epidemiol. Rec. 72: 97–100.

20. Zaki, M., and C. G. Clark. 2001. Isolation and characterization of polymorphic DNA from *Entamoeba histolytica*. J. Clin. Microbiol. 39(3): 897–905.

Received for publication 12 December 2007

Mammalian target of rapamycin and glycogen synthase kinase 3 differentially regulate lipopolysaccharide-induced interleukin-12 production in dendritic cells

Masashi Ohtani,[1,2] Shigenori Nagai,[1,2] Shuhei Kondo,[1] Shinta Mizuno,[1] Kozue Nakamura,[1] Masanobu Tanabe,[3] Tsutomu Takeuchi,[3] Satoshi Matsuda,[1,2] and Shigeo Koyasu[1,2]

[1]Department of Microbiology and Immunology, Keio University School of Medicine, Tokyo; [2]Core Research for Evolutional Science and Technology, Japan Science and Technology Agency, Saitama; and [3]Department of Tropical Medicine and Parasitology, Keio University School of Medicine, Tokyo, Japan

Phosphoinositide 3-kinase (PI3K) negatively regulates Toll-like receptor (TLR)–mediated interleukin-12 (IL-12) expression in dendritic cells (DCs). We show here that 2 signaling pathways downstream of PI3K, mammalian target of rapamycin (mTOR) and glycogen synthase kinase 3 (GSK3), differentially regulate the expression of IL-12 in lipopolysaccharide (LPS)–stimulated DCs. Rapamycin, an inhibitor of mTOR, enhanced IL-12 production in LPS-stimulated DCs, whereas the activation of mTOR by lentivirus-mediated transduction of a constitutively active form of Rheb suppressed the production of IL-12. The inhibition of protein secretion or deletion of IL-10 cancelled the effect of rapamycin, indicating that mTOR regulates IL-12 expression through an autocrine action of IL-10. In contrast, GSK3 positively regulates IL-12 production through an IL-10–independent pathway. Rapamycin-treated DCs enhanced Th1 induction in vitro compared with untreated DCs. LiCl, an inhibitor of GSK3, suppressed a Th1 response on *Leishmania major* infection in vivo. These results suggest that mTOR and GSK3 pathways regulate the Th1/Th2 balance though the regulation of IL-12 expression in DCs. The signaling pathway downstream of PI3K would be a good target to modulate the Th1/Th2 balance in immune responses in vivo. (Blood. 2008; 112:635-643)

Introduction

Dendritic cells (DCs) recognize pathogens via pattern-recognition receptors, such as Toll-like receptors (TLRs), nucleotide-binding oligomerization domain (NOD)-like receptors, and retinoic acid inducible gene-1 (RIG-I)-like receptors, produce various cytokines, including interleukin-12 (IL-12), and thus activate the innate immune system, which in turn leads to the induction of adaptive immunity.[1-5] Bioactive IL-12 is composed of p40 and p35 subunits and functions as a crucial inducer of Th1 responses. IL-12 is typically produced by antigen-presenting cells such as DCs and monocytes-macrophages and plays an important role in infection and tumor immunity.[1-5] Because the overproduction of IL-12 gives rise to strong cell-mediated immunity and organ-specific autoimmune diseases via exaggerated Th1 cell differentiation, it is critical that IL-12 levels be tightly controlled.[5]

Phosphoinositide 3-kinases (PI3Ks) are lipid kinases playing important roles in various signal transduction pathways.[6] PI3K family members are classified into 4 subgroups according to their structure and substrate specificity. Among them, class IA heterodimeric PI3Ks are involved in receptor-mediated signaling pathways in the immune system.[6,7] Phosphatidylinositol-(3,4)bisphosphate and phosphatidylinositol(3,4,5)trisphosphate produced by class IA PI3Ks recruit specific signaling proteins containing a pleckstrin homology domain to the plasma membrane. These proteins include Akt and phosphoinositide-dependent kinase 1 and are involved in a wide range of cellular responses, such as cell growth, survival, and cytokine production.[6,7] PI3K signaling pathways are counteracted by phosphatase and tensin homologue deleted on chromosome 10 (PTEN), a 3-phosphoinositide–specific lipid phosphatase.[6]

We have previously demonstrated that PI3K negatively regulates IL-12 production in DCs stimulated with TLR ligands.[8,9] An enhanced Th1 response was observed on *Leishmania major* infection,[8] and an impaired Th2 response was observed on *Strongyloides venezuelensis* infection[10] in mice deficient for p85α, a major regulatory subunit of class IA PI3K, indicating that PI3K plays a key role in the regulation of Th1/ Th2 balance in vivo. Although several reports confirmed the negative feedback regulation of IL-12 production by PI3K on TLR stimulation,[11-13] the molecular mechanism(s) remains controversial.

One downstream substrate of PI3K pathways is a Ser/Thr protein kinase named "mammalian target of rapamycin" (mTOR), which regulates cell growth and protein synthesis by activating p70 S6 kinase (p70S6K) and by inhibiting eukaryotic initiation factor 4E-binding protein 1 (4E-BP1).[14] There are 2 functionally distinct mTOR complexes, mTORC1 and mTORC2, and only mTORC1 acts downstream of the PI3K-Akt-tuberous sclerosis complex 2 (TSC2)–Rheb signaling pathway to phosphorylate p70S6K and 4E-BP1 in a rapamycin-sensitive fashion[14] (Figure 1A). Although the mTOR pathway is activated in response to not only growth factors but also environmental stresses such as hypoxia,[14] the TLR-triggered mTOR function is poorly understood. In the present study, we show that mTOR negatively regulates IL-12 production through the production of IL-10 in DCs. We further demonstrate that glycogen synthase kinase 3 (GSK3), another downstream target of PI3K pathways, is also involved in the PI3K-mediated regulation of IL-12 production in a manner distinct from that of mTOR. We also provide evidence that the inhibition of mTOR and

Submitted February 1, 2008; accepted April 9, 2008. Prepublished online as *Blood* First Edition paper, May 20, 2008; DOI 10.1182/blood-2008-02-137430.

The online version of this article contains a data supplement.

The publication costs of this article were defrayed in part by page charge payment. Therefore, and solely to indicate this fact, this article is hereby marked "advertisement" in accordance with 18 USC section 1734.

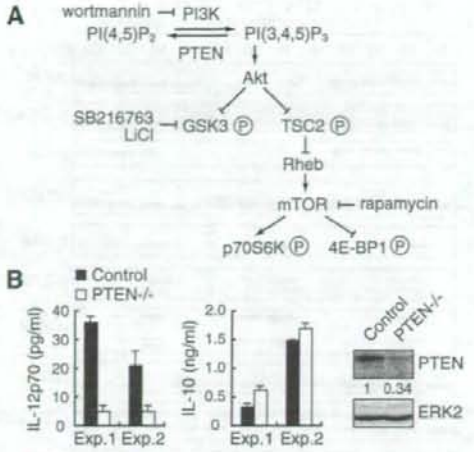

Figure 1. LPS-induced IL-12 production is suppressed in PTEN$^{-/-}$ BMDCs. (A) The overview of PI3K signaling pathway. $PI(4,5)P_2$ indicates phosphatidylinositol(4,5)bisphosphate; $PI(3,4,5)P_3$, phosphatidylinositol-(3,4,5)trisphosphate. (B) BMDCs from PTEN$^{-/-}$ mice (n = 2) or their littermate controls (n = 2) were stimulated with 1 μg/mL LPS for 24 hours and assayed for the production of IL-12p70 and IL-10 by ELISA. Data are indicated as median plus or minus SD. Essentially, the same results were obtained with 2 independent experiments (experiments 1 and 2). The expression levels of PTEN and ERK2 in BMDCs were determined by Western blotting (right panel).

GSK3 pathways in DCs results in the increase and decrease of Th1 responses, respectively.

Methods

Reagents

Lipopolysaccharide (LPS) from *Escherichia coli* 055:B5 was purchased from Sigma-Aldrich (St Louis, MO). Recombinant human (rh) GM-CSF, rhIL-4, rhIL-10, and recombinant mouse (rm) GM-CSF were purchased from PeproTech (Rocky Hill, NJ). Wortmannin, rapamycin, SB216763, cycloheximide, and brefeldin A (BFA) were purchased from Calbiochem (San Diego, CA). Antibodies to ERK2, IκBα, p70S6K, Rheb, GSK3α/β, and STAT3 were purchased from Santa Cruz Biotechnology (Santa Cruz, CA). Antibody to Akt and phosphorylation-specific antibodies to Akt (Ser473), GSK3α/β (Ser21/Ser9), TSC2 (Thr1462), p38 (Thr180/Tyr182), ERK (Thr202/Tyr204), JNK (Thr183/Tyr185), and STAT3 (Tyr705) were purchased from Cell Signaling Technology (Danvers, MA).

Mice

C57BL/6 and BALB/c mice were purchased from Nihon SLC. IL-10$^{-/-}$ mice on a C57BL/6 background were purchased from The Jackson Laboratory (Bar Harbor, ME). Mice deficient for p85α were reported previously.[15,16] Mice had been backcrossed to the BALB/c background for 12 generations. STAT3 mutant (LysM-Cre x STAT3$^{flox/flox}$) mice[17] on a mixed (129 × C57BL/6) background were kindly provided by Dr K. Takeda (Osaka University, Osaka, Japan). STAT3$^{flox/flox}$ or LysM-Cre x STAT3$^{flox/+}$ mice were used as controls. PTEN mutant (LysM-Cre x PTEN$^{flox/flox}$) mice[18,19] on a C57BL/6 background were kindly provided by Dr A. Suzuki (Akita University, Akita, Japan). PTEN$^{flox/flox}$ mice were used as controls. LysM-Cre x STAT3$^{flox/flox}$ and LysM-Cre x PTEN$^{flox/flox}$ mice were referred to here as STAT3$^{-/-}$ and PTEN$^{-/-}$ mice, respectively. Mice were maintained at Taconic Farms (Germantown, NY) or in our animal facility under specific pathogen-free conditions. All experiments were performed in accordance with our institutional guidelines.

Preparation of dendritic cells

To generate bone marrow (BM)–derived DCs (BMDCs), mouse BM cells were cultured at 10^6/mL in complete medium (RPMI 1640; Sigma-Aldrich, 10% fetal calf serum, 55 μM 2-mercaptoethanol, 100 U/mL penicillin, 100 μg/mL streptomycin) supplemented with 10 ng/mL rmGM-CSF for 6 days. The culture medium was changed every 2 days. On day 6, BMDCs were isolated using antimouse CD11c magnetic beads (Miltenyi Biotec, Auburn, CA) with an AutoMACS (Miltenyi Biotec). Human peripheral blood mononuclear cells from normal healthy volunteers were isolated by centrifugation on a Ficoll-Metrizoate density gradient (Lymphoprep; Nycomed, Oslo, Norway). The protocol was approved by the local ethics committee at Keio University School of Medicine, and informed consent was obtained from donors in accordance with the Declaration of Helsinki. Monocytes were then isolated using antihuman CD14 magnetic beads (Miltenyi Biotec) with an AutoMACS, followed by incubation at 10^6 cells/mL in complete medium supplemented with 100 ng/mL rhGM-CSF and 100 ng/mL rhIL-4 for 6 days, to obtain monocyte-derived DCs (MDDCs).

Western blotting

Western blotting was carried out as described.[8] To detect phospho-STAT3 and phospho-TSC2, immunoreaction enhancer (Can Get Signal, Toyobo, Japan) was added to the reaction according to the manufacturer's instructions. ERK2 was used as a loading control. A LAS-3000 imaging system (Fuji) was used to produce digital images. Signal intensities (for phospho-STAT3) and signal profiles (for p70S6K) were quantified with Image Gauge software version 4.1 (Fuji).

Enzyme-linked immunosorbent assay

Cytokine concentrations in the culture supernatants were quantified by enzyme-linked immunosorbent assay (ELISA; Quantikine; R&D Systems, Minneapolis, MN).

Quantitative real-time polymerase chain reaction

Total RNA was prepared using NucleoSpin RNA II (Macherey-Nagel, Düreu, Germany), and cDNA was synthesized with Ready-To-Go T-Primed First-Strand kit (GE Healthcare, Chalfont St Giles, United Kingdom). Quantitative real-time polymerase chain reaction (PCR) was performed by applying the real-time SYBR Green PCR technology using SYBR premix Ex Taq (Takara, Otsu, Japan) with specific primers on an iCycler IQ (Bio-Rad, Hercules, CA). PCR cycling was as follows: 95°C for 10 seconds for 1 cycle, 95°C for 5 seconds, 58°C for 20 seconds, 72°C for 15 seconds for 40 cycles, and 70°C for 5 minutes. Amplification of cyclophilin A mRNA was done for each sample as an endogenous control. Primer pairs specific for IL-12p40 (forward, CAGAAGCTAACCATCTCCTGGTTTG; reverse, CCGGAGTAATTTGGTGCTCCACAC), IL-12p35 (forward, TCACATCTCATCTCCCCAAA; reverse, TCTGCTAACACATTGAGGGG), IL-10 (forward, GGTTGCC-AAGCCTTATCGGA; reverse, ACCTGCTCCACTGCCTTGCT), interferon-β (IFN-β) (forward, CCATCCAAGAGATGCTCCAG; reverse, GTGGAGAGCAGTTGAGGACA), suppressor of cytokine signaling 3 (SOCS3) (forward, GGGGGAGGCAGGAGGTGATGGA; reverse, GGGCGGGCTGGAGGTGGATT) and cyclophilin A (forward, ATGGCACTGGCGGCAGGTCC; reverse, TTGCCATTCCTGGACCCAAA) were used.

Preparation of lentiviral vectors

The following constructs were kindly provided by Dr H. Miyoshi (RIKEN, Tsukuba, Japan): CSII-EF-MCS-IRES2-Venus, a self-inactivating lentiviral construct; pCAG-HIVgp and pCMV-VSVG-RSV-Rev, packaging constructs.[20] This lentiviral system is designed to express a desired gene under the direction of the elongation factor-1 promoter along with internal ribosomal entry site (IRES)-driven Venus, a derivative of YFP,[21] as a marker for monitoring the infection efficiency. Mouse Rheb was amplified by PCR using cDNA from the brain of C57BL/6 mice as a template (5′

primer, ATGCCTCAGTCCAAGTCCCG; 3′ primer, TCACATCACCGAGCACGAAG) and cloned into the pGEM-T Easy vector (Promega, Madison, WI). After sequence verification, the construct was subjected to PCR mutagenesis to obtain Rheb Q64L, a constitutively active form of Rheb, Glu-64 replaced by Leu. The product was verified by DNA sequencing and subcloned into CSII-EF-MCS-IRES2-Venus. For the generation of lentiviral vectors, 293T cells were transfected with CSII-EF-MCS-IRES2-Venus with or without Rheb Q64L insert, pCAG-HIVgp, and pCMV-VSUG-RSV-Rev using Lipofectamine 2000 (Invitrogen, Carlsbad, CA). After 2 days, culture supernatants were passed through a 0.45-μm filter, condensed to 0.5% volume, and used for gene transduction.

Generation of gene-transduced BMDCs

Mouse BM cells were incubated with phycoerythrin-conjugated antibodies against CD3ε, CD4, CD8α, CD11b, Gr-1, B220, and TER119 (BD Biosciences, San Jose, CA) along with anti-phycoerythrin microbeads (Miltenyi Biotec), followed by negative selection with an AutoMACS. The remaining cells (0.5×10^5 cells/0.5 mL) were cultured with 10 ng/mL rmGM-CSF in a 24-well plate for 2 days, followed by spin infection (1800 rpm, 2 hours) with 40 μL of each viral vector along with 5 μg/mL polybrene. After infection, each well was split into 2 wells (2 mL/well) and cultured with 10 ng/mL rmGM-CSF for another 4 days. The culture medium was changed every 2 days. The cells were then harvested, washed, and incubated with allophycocyanin-conjugated antimouse CD11c monoclonal antibody (mAb), and Venus-as well as CD11c-positive cells were sorted as gene-transduced BMDCs using a FACSAria (BD Biosciences). The purity was estimated to be more than 85%.

$CD4^+$ T-cell priming

Human MDDCs (1×10^6 cells) were incubated in the presence or absence of 10 μg/mL tuberculin purified protein derivative (PPD) for 1 hour, and subsequently stimulated with or without 1 μg/mL of LPS along with or without 100 nM of rapamycin. After 2 hours of stimulation, the cells were harvested, washed, and cultured (3×10^5 cells) for a week with $CD4^+$ T cells from the same donor (3×10^6 cells), which were isolated from peripheral blood mononuclear cells using antihuman CD4 magnetic beads (Miltenyi Biotec) with an AutoMACS. $CD4^+$ T cells were then restimulated with antihuman CD3ε (10 μg/mL) and antihuman CD28 (1 μg/mL) mAbs for 48 hours.

Leishmania major infection

L major infection was performed as described.[8,22] Two days after infection, 40 μL of 2 mM LiCl/phosphate-buffered saline (PBS) or PBS were injected into the infected left hind footpad subcutaneously.

Results

Products of PI3K are involved in the regulation of IL-12 expression

To prove that the lipid kinase activity of PI3K regulates IL-12 production, we examined the role of PTEN, which catalyzes a reaction opposite to PI3K (Figure 1A). BMDCs lacking PTEN produced lower amounts of IL-12 than control BMDCs on LPS stimulation (Figure 1B), indicating that the products of PI3Ks, phosphatidylinositol(3,4,5)trisphosphate in particular, are indeed critical for the regulation of IL-12 expression.

Activation of mTOR and GSK3 pathways by LPS stimulation of DCs

We examined the signaling components of PI3K-Akt pathway in LPS-stimulated BMDCs (Figure 1A). As shown in Figure 2, LPS stimulation induced the phosphorylation of TSC2 and GSK3,

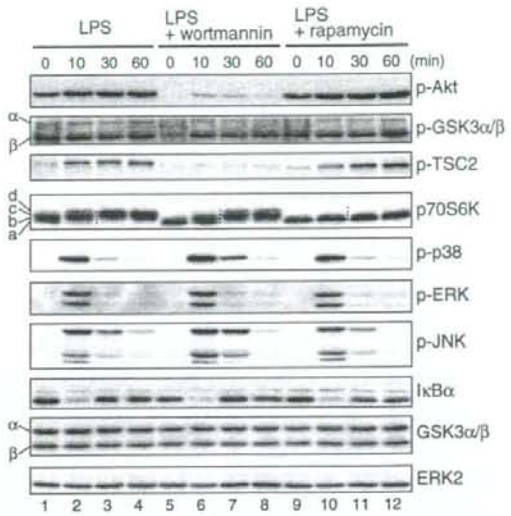

Figure 2. The PI3K signaling pathway is activated by LPS in BMDCs. BMDCs were cultured overnight and then pretreated with either 100 nM wortmannin or 10 ng/mL rapamycin for 20 minutes or left untreated before being stimulated with 1 μg/mL LPS for the indicated times. Cell lysates were analyzed for phospho-Akt, phospho-GSK3α/β, phospho-TSC2, p70S6K, phospho-p38, phospho-ERK, phospho-JNK, IκBα, GSK3α/β, and ERK2 by Western blotting. Four dots added between the 10-minute and 30-minute lanes of p70S6K samples indicate the migration positions of hyperphosphorylated p70S6K caused by multiple phosphorylation events, which are represented as a through d on the left side (Figure S1).

known targets of Akt. The activation of mTOR was evaluated by the phosphorylation of p70S6K. Consistent with the fact that mTOR is activated by serum and nutrients, p70S6K was partially phosphorylated even without LPS (Figure 2 lane 1). The hyperphosphorylation of p70S6K examined by electrophoretic mobility shifts was induced within 10 minutes (Figure 2 lane 2) and became clearer up to 60 minutes after LPS stimulation (Figure 2 and Figure S1 lane 4, available on the *Blood* website; see the Supplemental Materials link at the top of the online article; note that the electrophoretic mobility of p70S6K shifts from a and b up to c and d bands). Rapamycin completely blocked the phosphorylation of p70S6K (Figures 2, S1, compare lanes 1-4 and 9-12). In contrast, rapamycin had no effect on the LPS-induced phosphorylation of Akt and TSC2 (Figure 2 lanes 9-12), which is consistent with the fact that Akt and TSC2 act upstream of mTOR (Figure 1A). Wortmannin, an inhibitor of PI3K, only partially blocked the LPS-induced phosphorylation of p70S6K (Figures 2, S1, lanes 5-8), whereas the phosphorylation of Akt and TSC2 was completely inhibited (Figure 2 lanes 5-8). These data suggest that LPS-induced mTOR activation is mediated by both PI3K-dependent and-independent pathways, the latter of which could involve serum and/or nutrients.

GSK3 activity is negatively regulated by Akt-mediated phosphorylation.[23] We found that GSK3β was predominantly phosphorylated on LPS stimulation in BMDCs, whereas both GSK3α and GSK3β were expressed (Figure 2 lanes 1-4). The effect of wortmannin on GSK3β phosphorylation was partial (Figure 2 lanes 5-8), indicating that the LPS-induced phosphorylation of GSK3β was also mediated by both PI3K-dependent and -independent pathways. As expected, rapamycin had no effect on the LPS-induced phosphorylation of GSK3β (Figure 2 lanes 9-12).

We also examined the effects of rapamycin and wortmannin on LPS-activated MAPK and NF-κB pathways. Rapamycin had little effect on the phosphorylation status of MAPK family members or the degradation of IκBα, a measure of NF-κB activation (Figure 2, compare lanes 1-4 and lanes 9-12). In contrast, consistent with previous reports,[8,24,25] wortmannin slightly but reproducibly enhanced the LPS-induced phosphorylation of p38 as well as JNK (Figure 2, compare lanes 3 and 7), indicating that a PI3K-dependent but mTOR-independent pathway(s) negatively regulates the activation of p38 and JNK. Wortmannin had little effect on IκBα degradation, indicating that the NF-κB pathway is probably not the target of PI3K pathway in BMDCs.

Rapamycin augments LPS-induced IL-12 production but suppresses IL-10 production in an mTOR-dependent manner

We next examined the role of mTOR in the regulation of IL-12 expression. As shown in Figure 3A, the treatment of BMDCs with rapamycin as well as wortmannin enhanced LPS-induced IL-12p70 production. In contrast, LPS-induced IL-10 production was suppressed by rapamycin or wortmannin, and the effect of rapamycin was more potent than wortmannin (Figure 3A). Rapamycin had the same effect on human MDDCs (Figure S2). On the other hand, rapamycin and wortmannin had little effect on the production of IL-6 and tumor necrosis factor-α (TNF-α; Figure 3A). PTEN$^{-/-}$ BMDCs produced slightly more IL-10 compared with control BMDCs (Figure 1B), but the effect of PTEN deficiency is more pronounced on IL-12 compared with IL-10 production.

A complex of rapamycin and FK506-binding protein 12 (FKBP12) binds to and inhibits mTOR. Because FK506 competes with rapamycin for binding to FKBP12, the excess amounts of FK506 cancel the biologic actions of the rapamycin-FKBP12 complex.[26] Indeed, FK506 prevented the rapamycin-induced augmentation of IL-12p70 and IL-12p40 production in a dose-dependent manner (Figure 3B). The suppression of IL-10 production by rapamycin was also canceled with excess FK506 (Figures 3B, S3). Excess amounts of FK506 partially restored the hyperphosphorylation of p70S6K (Figure S3). These results confirm that the effect of rapamycin on cytokine production is mediated by the inhibition of mTOR function.

We further examined the effects of wortmannin and rapamycin on LPS-induced cytokine mRNA expression, including IL-12p40, IL-12p35, IL-10, and IFN-β by real-time RT-PCR (Figure 3C). Consistent with these results, the expression of both IL-12p40 and IL-12p35 mRNAs was enhanced by wortmannin and rapamycin. In contrast, IL-10 mRNA expression was suppressed only by rapamycin. Interestingly, wortmannin but not rapamycin enhanced LPS-induced IFN-β mRNA expression. These results collectively suggest that the PI3K regulates the expression of distinct sets of cytokine genes expression in mTOR-dependent and -independent pathways.

Constitutively active Rheb affects the regulation of cytokine production

To further confirm the role of mTOR in cytokine gene regulation, we used a lentiviral vector-mediated gene delivery system[20] to activate mTOR by expressing a constitutively active form of Rheb (Rheb Q64L).[27] The phosphorylation-induced electrophoretic mobility shift of p70S6K in untreated and LPS-stimulated DCs was augmented in BMDCs expressing Rheb Q64L compared with control BMDCs (Figure 4A and Figure S4 lanes 1 and 3, lanes 2 and 4), confirming the activity of Rheb Q64L. As shown in Figure

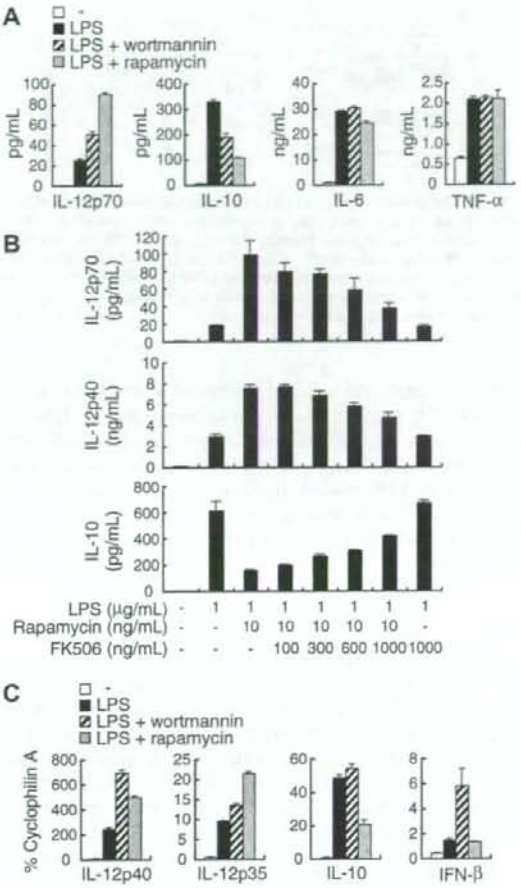

Figure 3. The effect of rapamycin on LPS-induced cytokine expression in BMDCs. (A) BMDCs were stimulated with 1 μg/mL LPS in the presence or absence of either 100 nM wortmannin or 10 ng/mL rapamycin for 24 hours and assayed for the production of IL-12p70, IL-10, IL-6, and TNF-α by ELISA. (B) BMDCs were stimulated with 1 μg/mL LPS with or without 10 ng/mL rapamycin along with the indicated concentrations of FK506 for 24 hours and assayed for the production of IL-12p70, IL-12p40, and IL-10 by ELISA. (C) BMDCs were pretreated with or without either 100 nM wortmannin or 10 ng/mL rapamycin for 20 minutes before stimulation with 1 μg/mL LPS. After 4 hours, total RNA was isolated, and IL-12p40, IL-12p35, IL-10, and IFN-β mRNA levels were assessed by real-time PCR using cyclophilin A mRNA as a reference. All data are indicated as median plus or minus SD of duplicate samples. Similar results were obtained with 2 to 4 independent experiments.

4B, LPS-induced IL-12p70 production was decreased in Rheb Q64L-expressing BMDCs compared with mock-infected BMDCs. In contrast, LPS-induced IL-10 production was increased in Rheb Q64L-expressing BMDCs. No difference in IL-6 production was observed (data not shown). These results indicate that mTOR is indeed involved in the regulation of IL-12 and IL-10 production in LPS-stimulated BMDCs.

The effect of rapamycin on IL-12 expression involves IL-10 in an autocrine manner

Because mTOR is involved in diverse biologic processes, including protein synthesis and gene expression,[14] it is possible that mTOR regulates IL-12 gene expression through new protein synthesis. When BMDCs were treated with cycloheximide to inhibit de novo

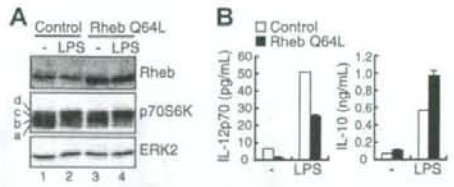

Figure 4. The effect of Rheb Q64L on LPS-induced cytokine production. BMDCs were infected with a lentivirus vector expressing a constitutively active form of Rheb (Rheb Q64L) or vector alone (control). Gene-transduced BMDCs were isolated ("Methods") and stimulated with or without 1 μg/mL LPS for 24 hours. (A) The cell lysates were analyzed for Rheb, p70S6K, and ERK2 by Western blotting. Note that the mobility shifts of p70S6K caused by multiple phosphorylation are represented as a through d (Figure S4). (B) The production of IL-12p70 and IL-10 in culture supernatants was assayed by ELISA.

protein synthesis, the effect of rapamycin was reduced (data not shown). BFA, which blocks protein secretion, abrogated the effect of rapamycin on LPS-induced IL-12p40 and IL-12p35 mRNA expression (Figure 5A). These results strongly suggest that rapamycin controls LPS-induced IL-12 expression through a newly synthesized autocrine mediator(s).

IL-10 is an anti-inflammatory cytokine capable of inhibiting the LPS-induced production of proinflammatory cytokines, including IL-12 in DCs.[28] When we examined the kinetics of LPS-induced IL-12 and IL-10 expression, rapamycin augmented IL-12p40 and IL-12p35 mRNA expression at 4 hours but not 2 hours after LPS stimulation (Figure 5B). On the other hand, the rapamycin-induced suppression of IL-10 mRNA expression was already observed at 2 hours after LPS stimulation (Figure 5B). Consistent with these results, LPS-induced IL-10 production evaluated by ELISA was significantly reduced by rapamycin at 4 hours after LPS stimulation, whereas IL-12p40 production was little affected (data not shown). These results suggest that the suppression of IL-10 expression by rapamycin subsequently augments IL-12 expression.

To test this hypothesis further, we examined whether rapamycin attenuates the IL-10 signaling pathway in LPS-stimulated DCs. For this purpose, we analyzed the phosphorylation status of STAT3 at Tyr705 as a measure of IL-10 signaling. We found that the tyrosine phosphorylation of STAT3 was markedly induced at 2 hours after LPS stimulation, which was inhibited by rapamycin (Figure 5C). Similar results were obtained in human MDDCs (Figure S5). To rule out the possibility that rapamycin directly inhibits the STAT3 signaling pathway, we examined the effect of rapamycin on the IL-10–induced expression of SOCS3, a well-known target of the STAT3 signaling pathway.[29] As shown in Figure 5D, SOCS3 mRNA expression induced by IL-10 stimulation was unaffected by rapamycin. Collectively, these results indicate that rapamycin directly suppresses LPS-induced IL-10 expression but not the STAT3 signaling pathway.

To confirm that rapamycin works through the IL-10-STAT3 pathway to down-regulate IL-12 expression, we used IL-$10^{-/-}$ and STAT$3^{-/-}$ DCs. As shown in Figure 5E, the effect of rapamycin was virtually absent in IL-$10^{-/-}$ BMDCs (1.2 ± 0.03-fold increase) compared with WT BMDCs (3.8 ± 0.1-fold increase). Essentially the same result was obtained with STAT$3^{-/-}$ BMDCs (Figure 5F, 3.3 ± 0.2-fold increase in control BMDCs vs 1.2 ± 0.1-fold increase in STAT$3^{-/-}$ BMDCs). The production of IL-12p70 from IL-$10^{-/-}$ DCs was strongly suppressed by the addition of exogenous IL-10, and such inhibition was rapamycin-independent (Figure S6). These results clearly indicate that rapamycin enhances IL-12 production through the inhibition of autocrine IL-10 action in LPS-stimulated BMDCs.

mTOR and GSK3 cooperatively regulate LPS-induced IL-12 production

As wortmannin had only a marginal effect on LPS-induced phosphorylation of p70S6K (Figure 2) as well as IL-10 expression (Figure 3A,C), we examined pathways other than mTOR that lie downstream of PI3K. Indeed, GSK3 has been reported to regulate the TLR-mediated production of cytokines, such as IL-12p40 and IL-10 in human monocytes and DCs.[30,31] We therefore examined whether GSK3 regulates LPS-induced cytokine production in mouse BMDCs using SB216763, a specific GSK3 inhibitor. SB216763 attenuated IL-12p70 production but enhanced IL-10 production by LPS-stimulated DCs (Figure 6A, lane 5). We obtained similar results with another GSK3 inhibitor LiCl (data not shown). These data indicate that PI3K regulates IL-12 production through both mTOR and GSK3 pathways and that GSK3 positively regulates LPS-induced IL-12p70 and negatively regulates IL-10 production in BMDCs.

Given that the PI3K-Akt pathway negatively regulates GSK3 (Figure 1A), the treatment of cells with wortmannin should activate GSK3. Interestingly, wortmannin augmented the effect of rapamycin on LPS-induced IL-12p70 production (Figure 6A lanes 2-4 and 6). On the other hand, consistent with the marginal effect of wortmannin alone (Figure 6A lane 3), wortmannin failed to augment the suppressive effect of rapamycin on LPS-induced IL-10 production (Figure 6A lanes 2-4 and 6), suggesting that mTOR and GSK3 differentially regulate IL-12 production. Wortmannin had little effect on LPS-induced IL-12p70 and IL-10 production in the presence of SB216763 (Figure 6A lanes 5 and 7). It is probable that the contribution of GSK3 is similar to or greater than that of mTOR for the regulation of IL-12 production in DCs. Consistent with those observations, LPS-induced IL-12p70 production was decreased in the presence of SB216763 in IL-$10^{-/-}$ BMDCs (Figure 6B). These results collectively indicate that GSK3 directly regulates LPS-induced IL-12 production independent of IL-10 (Figure 6C).

Attenuation of mTOR and GSK3 affects Th1/Th2 balance

Because IL-12 is critical for triggering Th1 responses, our results raise an interesting possibility that blocking mTOR and GSK3 may enhance and diminish Th1 responses, respectively. Human peripheral $CD4^+$ T cells stimulated with MDDCs pretreated with LPS plus PPD in the presence of rapamycin produced more IFN-γ on restimulation with anti-CD3 plus anti-CD28 antibodies than $CD4^+$ T cells stimulated with DCs pretreated in the absence of rapamycin (Figure 7A). It is thus probable that treatment of DCs with rapamycin results in the augmentation of a Th1 response presumably through enhanced IL-12 production and reduced IL-10 production. We next examined the effect of GSK3 inhibition in an in vivo infection model with *L major*, in which adequate Th1 development is required for disease control.[22] We have previously shown that Th2 prone BALB/c mice can elicit a reasonable Th1 response on *L major* infection in the absence of p85α (Fukao et al[8] and Figure 7B, compare open triangles and open circles). Because GSK3 is expected to have an increased activity in the absence of p85α, we administered a GSK3 inhibitor, LiCl, into footpad of p85α$^{-/-}$ mice on a BALB/c background when infected with *L major*. As shown in Figure 7B, whereas p85α$^{-/-}$ BALB/c mice were resistant to infection, the administration of LiCl to p85α$^{-/-}$ BALB/c mice resulted in increased footpad swelling and animals were no longer able to control the infection. These results

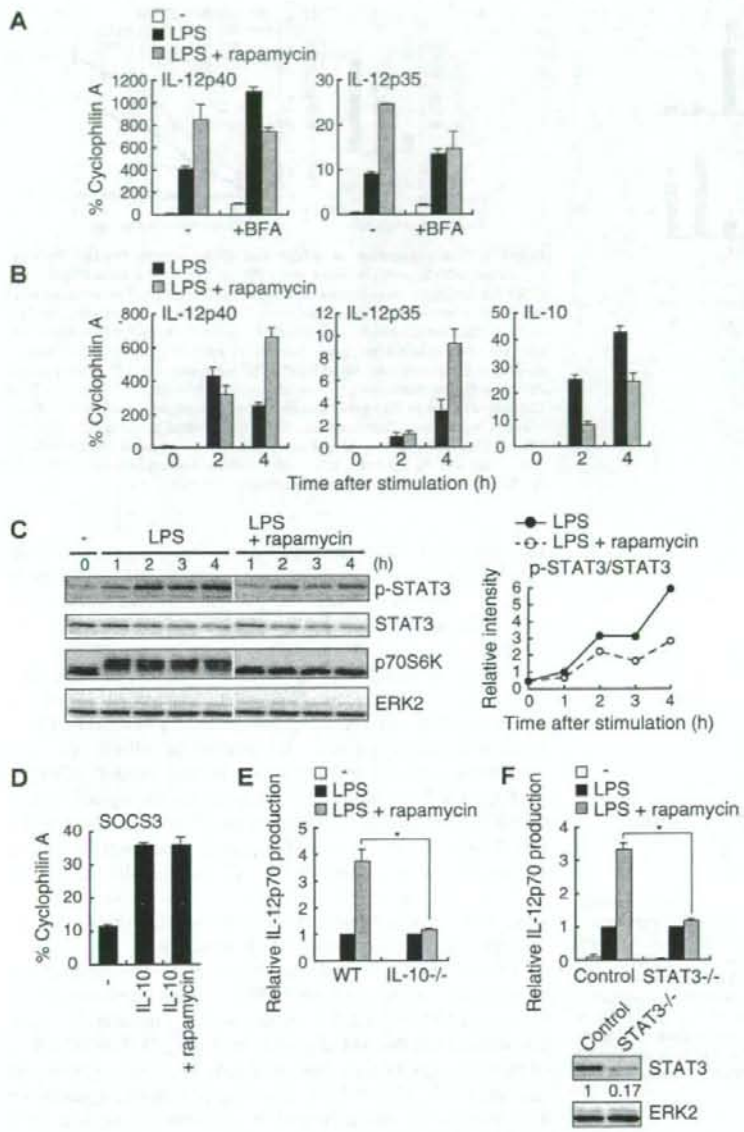

Figure 5. The effect of rapamycin on LPS-induced IL-12 production depends on the IL-10–STAT3 signaling pathway. (A) BMDCs were pretreated with or without 10 ng/mL rapamycin along with or without 5 μg/mL BFA for 20 minutes before stimulation with 1 μg/mL LPS. After 4 hours, total RNA was isolated, and IL-12p40 and IL-12p35 mRNA levels were assessed by real-time PCR using cyclophilin A mRNA as a reference. (B) BMDCs were pretreated with or without 10 ng/mL rapamycin for 20 minutes and then stimulated with 1 μg/mL LPS for the indicated times. Total RNA was isolated, and IL-12p40, IL-12p35, and IL-10 mRNA levels were assessed by real-time PCR using cyclophilin A mRNA as a reference. (C) BMDCs were pretreated with or without 100 ng/mL rapamycin for 20 minutes and then stimulated with 1 μg/mL LPS for the indicated times. The cell lysates were analyzed for phospho-STAT3, STAT3, p70S6K, and ERK2 by Western blotting. The white lines indicate that intervening lanes have been removed. The right panel indicates relative intensities of tyrosine-phosphorylated STAT3 normalized by STAT3 signals. (D) BMDCs were pretreated with or without 100 ng/mL rapamycin for 20 minutes before stimulation with 10 ng/mL IL-10. After 1 hour, total RNA was isolated, and SOCS3 mRNA levels were assessed by real-time PCR using cyclophilin A mRNA as a reference. In panels A, B, and D, data are indicated as mean plus or minus SD of duplicate samples. Data are representative of 2 (B,C) or 3 (A,D) independent experiments with similar results. (E) BMDCs from WT or IL-10$^{-/-}$ mice were stimulated with 1 μg/mL LPS in the presence or absence of 10 ng/mL rapamycin for 24 hours and assayed for the production of IL-12p70 by ELISA. Absolute IL-12p70 levels in the stimulation of LPS alone: WT, 24.1 plus or minus 3.6 pg/mL; IL-10$^{-/-}$, 1120 plus or minus 230 pg/mL. Data are indicated as median plus or minus SD of 3 independent experiments. *$P < .05$ by Mann-Whitney U test comparing WT with IL-10$^{-/-}$ groups. (F) BMDCs from STAT3$^{-/-}$ mice or littermate controls were stimulated with 0.1 μg/mL LPS in the presence or absence of 100 ng/mL rapamycin for 24 hours. Cytokine production was evaluated as in panel E. Absolute IL-12p70 levels in the stimulation of LPS alone: control, 11.8 plus or minus 3.7 pg/mL; STAT3$^{-/-}$, 299 plus or minus 67 pg/mL. *$P < .05$ by Mann-Whitney U test comparing control with STAT3$^{-/-}$ groups. Indicated below are the expression levels of STAT3 and ERK2 in BMDCs determined by Western blotting.

collectively indicate that the attenuation of mTOR and GSK3 by inhibitors affects the balance between Th1 and Th2 responses.

Discussion

We have previously shown that PI3K negatively regulates TLR-induced pro-inflammatory cytokine production by DCs and gut epithelial cells.[8,9,25] Because LPS-induced IL-12 production was decreased in PTEN$^{-/-}$ BMDCs (Figure 1B), the PI3K-Akt pathway triggered by the lipid product of PI3K is indeed important for the suppression of LPS-induced IL-12 production.

Furthermore, our results show that the PI3K-Akt pathway positively regulates IL-10 production. IL-10 is produced by various cell types and plays anti-inflammatory roles in many immune responses.[32] In particular, it has been shown that DC-derived IL-10 is involved in a variety of responses, such as infectious diseases,[33] the induction of tolerance,[34] and cytotoxic T-lymphocyte–mediated antitumor activity.[32] Considering that IL-10 plays a pivotal role in immune regulation, the elucidation of the molecular mechanism underlying PI3K-mediated IL-10 regulation would shed new light on therapeutic approaches toward cancer as well as autoimmune diseases.

Indeed, signaling molecules involved in the PI3K pathway (ie, mTOR and GSK3) seem reasonable targets for appropriately modulating the Th1/Th2 balance. As shown here, the treatment of DCs with rapamycin augments a Th1 response (Figure 7A). Because rapamycin does not alter antigen uptake

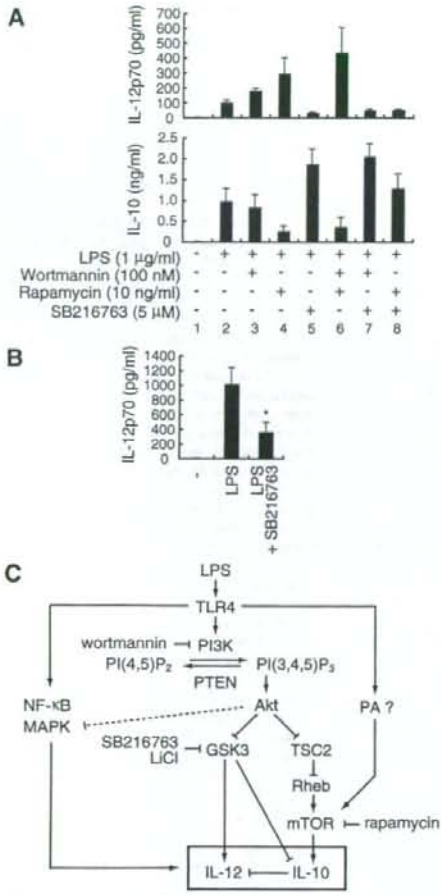

Figure 6. mTOR and GSK3β regulate LPS-induced IL-12 production through distinct mechanisms. (A) BMDCs were stimulated with 1 μg/mL LPS together with the indicated inhibitors for 24 hours and assayed for the production of IL-12p70 and IL-10 by ELISA. Data are indicated as median plus or minus SD of 3 independent experiments. (B) BMDCs from IL-10$^{-/-}$ mice were stimulated with 1 μg/mL LPS in the presence or absence of 5 μM SB216763 for 24 hours and assayed for the production of IL-12p70 by ELISA. Data are indicated as median plus or minus SD of 5 independent experiments. *$P < .05$ by Wilcoxon *t* test compared with LPS alone. (C) The schematic diagram of the PI3K-mediated regulation of IL-12 production. PA indicates phosphatidic acid; $PI(4,5)P_2$, phosphatidylinositol(4,5)bisphosphate; $PI(3,4,5)P_3$, phosphatidylinositol(3,4,5)trisphosphate.

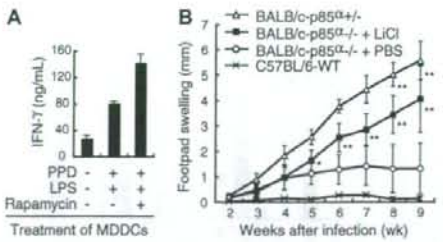

Figure 7. The attenuation of mTOR and GSK3 affects Th1/Th2 balance. (A) Human MDDCs were pretreated with PPD and LPS with or without rapamycin. CD4$^+$ T cells from the same donor were cultured with those MDDCs in the absence of rapamycin. After 1 week of incubation, CD4$^+$ T cells were stimulated with anti-CD3ε and anti-CD28 mAbs for 48 hours and assayed for the production of IFN-γ by ELISA. Data are indicated as median plus or minus SD of duplicate samples. (B) The footpad swelling of *L major*–infected BALB/c-p85α$^{-/-}$ mice treated with LiCl ($n = 8$) or with PBS ($n = 6$) was monitored on a weekly basis. BALB/c-p85α$^{+/-}$ mice ($n = 5$) or C57BL/6-WT mice ($n = 2$) were used as positive and negative controls for *L major* infection, respectively. Data are indicated as median plus or minus SD. *$P < .05$, **$P < .01$ by Mann-Whitney U test compared with PBS-treated BALB/c-p85α$^{-/-}$ mice. There was no significant difference in footpad swelling between LiCl-treated BALB/c-p85α$^{-/-}$ mice and untreated BALB/c-p85α$^{+/-}$ mice.

and presentation,[35] or the expression level of costimulatory molecules such as CD80 and CD86 in DCs,[36] the enhancement of a Th1 response by rapamycin is probably the result of the augmentation of IL-12 production. In addition, the inhibition of GSK3 by LiCl suppressed a Th1-mediated immune response against *L major* in vivo (Figure 7B). These results raise the possibility that the attenuation of these signaling pathways may provide new therapeutic approaches for human diseases.

Based on our present studies as well as other reports, we propose that signal transduction pathways downstream of Akt regulating IL-12 production are composed of at least 3 components: mTOR, GSK3, and MAPK (Figure 6C). First, the mTOR pathway negatively regulates IL-12 production through the induction of IL-10 gene expression. Wortmannin did not completely inhibit the LPS-induced phosphorylation of p70S6K (Figure 2), and a combination of wortmannin and rapamycin further enhanced LPS-induced IL-12 production (Figure 6A), suggesting that the LPS-induced mTOR activation depends only partially on the PI3K pathway. It should be noted that phosphatidic acid produced by LPS stimulation in macrophages activates mTOR in a PI3K-independent manner[37] (Figure 6C).

Second, the GSK3 pathway positively regulates IL-12 production in a more direct manner. Using human monocytes, Martin et al[30] showed that GSK3 positively regulates LPS-induced IL-12p40 production. GSK3 augments the binding of NF-κB p65 to a coactivator "cAMP response element-binding protein" (CREB)-binding protein by competitively inhibiting the binding of CREB to CREB-binding protein.[30] Rodionova et al[31] have also shown that GSK3 enhances IL-12p70 and IL-12p40 production by human *Escherichia coli*–activated MDDCs. Considering that the GSK3-mediated regulation of IL-12 production was independent of IL-10 (Figure 6B), it is probable that GSK3 controls LPS-induced IL-12 production by a mechanism distinct from mTOR.

Third and finally, we and others have reported that the treatment of monocytes or DCs with SB203580, a specific inhibitor of p38, suppressed LPS-induced IL-12 production.[8,11,38] In addition, consistent with the fact that Akt negatively regulates p38,[39] the inhibition of PI3K during LPS activation enhanced p38 phosphorylation and activation[8,24,25] (Figure 2). Conversely, p38 phosphorylation on LPS stimulation was decreased in macrophages derived from PTEN$^{-/-}$ mice.[40] These observations suggest that the PI3K-mediated suppression of p38 results in the attenuation of IL-12 production as well. It has also been reported that the PI3K-Akt pathway negatively regulates JNK activity.[41] Indeed, the treatment of BMDCs with wortmannin slightly enhanced LPS-induced JNK phosphorylation (Figure 2). Studies regarding the function of JNK in LPS-induced IL-12 production using human monocyte cell lines are controversial,[42,43] and the role of JNK in LPS-induced IL-12 production should be evaluated in primary cells, such as BMDCs derived from JNK-deficient mice. Given that rapamycin (Figure 2) and SB216763 (data not shown) had no effect on LPS-induced phosphorylation of p38 and JNK, it seems improbable that mTOR or GSK3 is involved in the PI3K-Akt pathway-mediated negative regulation of p38 and JNK activity. These results taken together indicate that mTOR, GSK3, and MAPK cooperatively regulate TLR-induced IL-12 production in DCs (Figure 6C).

In contrast to IL-10, IFN-β enhances IL-12 production in an autocrine manner.[44] Because wortmannin augments the expression of IFN-β in response to LPS (Figure 3C), it is possible that wortmannin enhances IL-12 production through IFN-β. However, whereas wortmannin enhances the expression of both IL-12p40 and IL-12p35, IFN-β enhances the expression of IL-12p35 but not IL-12p40,[44] suggesting that the effect of wortmannin is probably not mediated by IFN-β. In contrast to wortmannin, rapamycin affected only IL-10 but not IFN-β gene expression (Figure 3C).

Because IL-10 inhibits the LPS-induced production of a diverse array of cytokines, such as IL-6 and TNF-α in addition to IL-12,[28] rapamycin may influence the production of these cytokines. However, we found that rapamycin had no effect on LPS-induced IL-6 and TNF-α production (Figure 3A), consistent with a previous observation that the LPS-induced mRNA expression of IL-12p40, but not TNF-α, is decreased in BMDCs expressing a constitutively active STAT3.[45] Although not shown, rapamycin also augmented IL-12p40 production and suppressed IL-10 production in mouse BMDCs in response to other TLR ligands, such as zymosan (for TLR2/6) and CpG-ODN (for TLR9), whereas it had no effect on IL-6 production. It is possible that the expression of those cytokines has different sensitivities to the negative regulation by IL-10.

What is the molecular mechanism underlying the PI3K-mediated regulation of LPS-induced IL-10 production? p70S6K, one of the targets regulated by mTOR, is able to increase the translation of a subset of mRNAs that contain a 5′ tract of oligopyrimidine.[46] However, the 5′ tract of oligopyrimidine was not detected in mouse or human IL-10 mRNA. Another target molecule, 4E-BP1, regulates eIF-4E, which stimulates translational initiation but whose function is thought to be general and not restricted to a subset of genes. mTOR is also involved in gene transcription through the regulation of transcriptional factors without a translational event.[14,47,48] This mechanism is more probable because our observations indicate that rapamycin suppresses LPS-induced IL-10 production at a transcriptional level (Figure 3C), rather than through translational regulators. However, the DNA binding of transcriptional factor Sp1 to the *IL10* promoter in LPS-stimulated mice BMDCs was unaffected in the presence of rapamycin (data not shown). The regulation by transcription factors downstream of mTOR remains to be elucidated in future studies. In addition to mTOR, GSK3 is involved in a regulatory pathway for IL-10 production. Indeed, GSK3 negatively regulated LPS-induced IL-10 production (Figure 6A), presumably by inactivation of CREB,[30] which is involved in the transcriptional activation of the *IL10* gene.

It should be noted that many previous studies on the regulation of IL-10 or IL-12 gene expression were performed using macrophage or DC cell lines. We have been aware that cell lines and primary cells often showed different results. One obvious problem is the fact that many cell lines have some defect or alteration in PI3K-PTEN regulation, such that many immortalized cell lines lack PTEN expression and show enhanced Akt activity. These cells are obviously not suitable for studying PI3K pathways. Detailed analysis with primary cells is important in future studies.

Acknowledgments

The authors thank Drs A. Suzuki, H. Miyoshi, and K. Takeda for valuable materials, Dr T. Luft of German Cancer Research Center for valuable discussion and sharing unpublished data, and Dr Linda K. Clayton of Harvard Medical School for critically reading the manuscript.

This work was supported by the Uehara Memorial Foundation, a Keio Gijuku Academic Development Fund (S. Matsuda), a Grant-in-Aid for Scientific Research (C 19590499; S. Matsuda) from the Japan Society for the Promotion of Science, a Grant-in-Aid for Scientific Research on Priority Areas (14021110 and 18073015), a National Grant-in-Aid for the Establishment of a High-Tech Research Center in a private university, and a Scientific Frontier Research Grant from the Ministry of Education, Culture, Sports, Science and Technology, Japan.

Authorship

Contribution: M.O. designed the research, performed experiments, and wrote the paper; S.N., S. Kondo, S. Mizuno, K.N., and M.T. performed experiments; T.T. and S. Matsuda designed the research; and S. Koyasu designed the research and wrote the paper.

Conflict-of-interest disclosure: The authors declare no competing financial interests.

Correspondence: Shigeo Koyasu, Department of Microbiology and Immunology, Keio University School of Medicine, 35 Shinanomachi, Shinjuku-ku, Tokyo 160-8582, Japan; e-mail: koyasu@sc.itc.keio.ac.jp.

References

1. Banchereau J, Briere F, Caux C, et al. Immunobiology of dendritic cells. Annu Rev Immunol. 2000; 18:767-811.
2. Steinman RM, Hemmi H. Dendritic cells: translating innate to adaptive immunity. Curr Top Microbiol Immunol. 2006;311:17-58.
3. Takeda K, Kaisho T, Akira S. Toll-like receptors. Annu Rev Immunol. 2003;21:335-376.
4. Creagh EM, O'Neill LA. TLRs, NLRs and RLRs: a trinity of pathogen sensors that co-operate in innate immunity. Trends Immunol. 2006;27:352-357.
5. Trinchieri G. Interleukin-12 and the regulation of innate resistance and adaptive immunity. Nat Rev Immunol. 2003;3:133-146.
6. Vanhaesebroeck B, Leevers SJ, Ahmadi K, et al. Synthesis and function of 3-phosphorylated inositol lipids. Annu Rev Biochem. 2001;70:535-602.
7. Koyasu S. The role of PI3K in immune cells. Nat Immunol. 2003;4:313-319.
8. Fukao T, Tanabe M, Terauchi Y, et al. PI3K-mediated negative feedback regulation of IL-12 production in DCs. Nat Immunol. 2002;3:875-881.
9. Fukao T, Koyasu S. PI3K and negative regulation of TLR signaling. Trends Immunol. 2003;24:358-363.
10. Fukao T, Yamada T, Tanabe M, et al. Selective loss of gastrointestinal mast cells and impaired immunity in PI3K-deficient mice. Nat Immunol. 2002;3:295-304.
11. Goodridge HS, Harnett W, Liew FY, Harnett MM. Differential regulation of interleukin-12 p40 and p35 induction via Erk mitogen-activated protein kinase-dependent and -independent mechanisms and the implications for bioactive IL-12 and IL-23 responses. Immunology. 2003;109:415-425.
12. Martin M, Schifferle RE, Cuesta N, Vogel SN, Katz J, Michalek SM. Role of the phosphatidylinositol 3 kinase-Akt pathway in the regulation of IL-10 and IL-12 by Porphyromonas gingivalis lipopolysaccharide. J Immunol. 2003;171:717-725.
13. Kuo CC, Lin WT, Liang CM, Liang SM. Class I and III phosphatidylinositol 3′-kinase play distinct roles in TLR signaling pathway. J Immunol. 2006; 176:5943-5949.
14. Wullschleger S, Loewith R, Hall MN. TOR signaling in growth and metabolism. Cell. 2006;124: 471-484.
15. Suzuki H, Terauchi Y, Fujiwara M, et al. Xid-like immunodeficiency in mice with disruption of the p85alpha subunit of phosphoinositide 3-kinase. Science. 1999;283:390-392.
16. Terauchi Y, Tsuji Y, Satoh S, et al. Increased insulin sensitivity and hypoglycaemia in mice lacking the p85 alpha subunit of phosphoinositide 3-kinase. Nat Genet. 1999;21:230-235.
17. Takeda K, Clausen BE, Kaisho T, et al. Enhanced Th1 activity and development of chronic enterocolitis in mice devoid of Stat3 in macrophages and neutrophils. Immunity. 1999; 10:39-49.
18. Clausen BE, Burkhardt C, Reith W, Renkawitz R,